# CHAPTER III

# RESULTS AND DISCUSSIONS

## 3.1  Reversed Flow Injection Analysis Determination of Chlortetracycline

Various methods were proposed for determination of chlortetracycline (CTC) in a variety of CTC samples such as HPLC with various detectors such as UV detector [193-197], fluorescence [198-200], MS [201-204], and electrochemical detector [205-206]. In recent year, micellar liquid chromatographic (MLC) technique has been proposed as a means for the development of greener analytical technique [207]. These analytical methods are included on the chromatographic analyses that appear in comprehensive review [208]. However, some of these methods still cause some problems for improvement from the point of recovery and reproducibility that has also been reported by other authors. It is therefore recommended to use SPE cartridges and LC analytical columns containing a high purity silica or polymer materials for separation proposes [209].

Several flow injection analysis (FIA) methods for pharmaceutical assays have been reported in recent reviews [210,211] because the requirements demanded by pharmaceutical industries concerning automation and higher sampling rate therefore the flow system with various detectors have been developed. Amperometric flow systems were described [212-214]. They are high analytical sensitivity but accomplish low sample throughput. Chemiluminescence (CL) flow systems were a better alternative, they required suitable CL reagents and oxidants. Various oxidizing agents used in CL reactions such as lucigenin or hexacyanoferrate [215], bromine

[216], $[Cu(HIO_6)_2]^{5-}$ [217] and silver(II) ion [218] were reported. In these CL systems, some of the oxidants are unstable, owing to their stronger oxidizing power that can oxidize a large number of inorganic and organic substances, expensive and the oxidizing reagents used are highly toxic.

Most spectrophotometric detection for the determination of CTC are based on its abilities to bind with metals, such as iron (III) [219, 220], copper (II) [221], magnesium (II) [222, 223] and some lanthanide ions, especially those of europium [224], indium [225] and terbium [226]. Since the conventional spectrophotometric methods for CTC determinations are tedious and time consuming. Flow injection analysis (FIA) methods with spectrophotometric detections have been employed instead [227, 228]. Otherwise, these methods are indirect detection therefore they present as main disadvantages their application to a very limited concentration range, the need of a compensation procedure for the measurements due to the samples intrinsic color. Recently, the use of micelles in analytical chemistry involving the beneficial alteration of metal ion – ligand complex spectral properties via surfactant association is growing [329-234 ]. Normally, the metal – complexes formed in the micellar systems, a pseudo – single – phase formed by surfactant micelles in an aqueous solution, are more stable than those formed in the absence of micelles. The size of micelles provided the equilibrium to be attained quickly with a change in pH. Currently, surfactant system used in development of many spectrophotometric methods for determining micro amounts of metal ions to improve the sensitivity for these methods [235].

This work describes a reversed flow injection analysis (rFIA) for CTC determination in which a small volume of reagent solution is injected into a sample

and carrier streams. Because the reagent bolus increases with increasing dispersion, the determination is carried out with only slight dilution [236]. The determination of CTC based on the reaction between yttrium (III) with CTC forming a colored complex and followed by spectrophometric detection was carried out. In order to avoid the limitation of the spectrophotometric detection, cetyltrimethylammonium bromide (CTAB) surfactant was used as a micellar medium for this complex to enhance the sensitivity of the method. Moreover, an effort was also made to develop a rapid, sensitive and reproducible method for this drug determination. Various factors influencing the sensitivity of this method were optimized by using both univariate and simplex methods

### 3.1.1 Manifold Design

The manifold is usually consisting of all parts of the system that contribute to the dispersion which will be restricted to mean the tubing, coils, connecting pieces, confluence point, etc. The real dispersion effects are due to the manifold designed in conjunction with the flow rate of the carrier stream and sample volume.

A simple reverse flow injection method for the determination of chlortetracycline (CTC) has been developed. It is based on the reaction between chlortetracycline with yttrium (III) in Tris (hydroxymethyl) aminomethane (Tris-buffer) and cationic surfactant medium. The chemical and FIA parameters were investigated using the univariate and simplex methods. The method involved injection yttrium (III) in CTAB solution into merged stream of sample and/or standard solution containing CTC and Tris – buffer. The resulting yellow complex with a maximum absorption at 392 nm was measured spectrphotometrically..

Two designs of the rFI manifolds were fabricated (Fig. 3.1). The first designed FI maniflold was a 2 channels manifold (Fig. 3.1A) in which the 2 solutions (Tris-buffer and sample/standard line) were flow through the rFIA system with the same flow rate. The reagent (yttrium solution) was injected into the stream of Tris buffer line via an injection valve and merged with the sample or standard CTC stream then all solutions were passed through a mixing coil to permit effective mixing and reached the flow cell of the spectrophotometric detector where measurements were made. Another designed (Fig.3.1B) was similar to the first one but the injection of reagent (yttrium solution) was made by inserting to the merged streams of Tris-buffer solution and sample/standard solution.

The results are shown in Table 3.1. It was found that, the injection of reagent into the merged streams (Fig. 3.1B) was satisfactory, in term of peak height and sensitivity, rather than injecting into the buffer stream before merging (Fig. 3.1A). The appropriate rFI manifold chosen was shown in Fig. 3.1B.

**Table 3.1** Effect of type of manifold on peak height

| Type of Manifold | Net signal * (Absorbance unit) obtained from the standard CTC( x $10^{-5}$ mol $l^{-1}$) | | | | | y = a(x)+b | $R^2$ |
|---|---|---|---|---|---|---|---|
| | 1.000 | 2.000 | 3.000 | 4.000 | 5.000 | | |
| A | 0.0094 | 0.0102 | 0.0114 | 0.0132 | 0.0140 | y = 121.89x + 0.008 | 0.9824 |
| B | 0.0096 | 0.0120 | 0.0138 | 0.0155 | 0.0167 | y = 180.45x + 0.008 | 0.9852 |

* Average of three replicate determinations
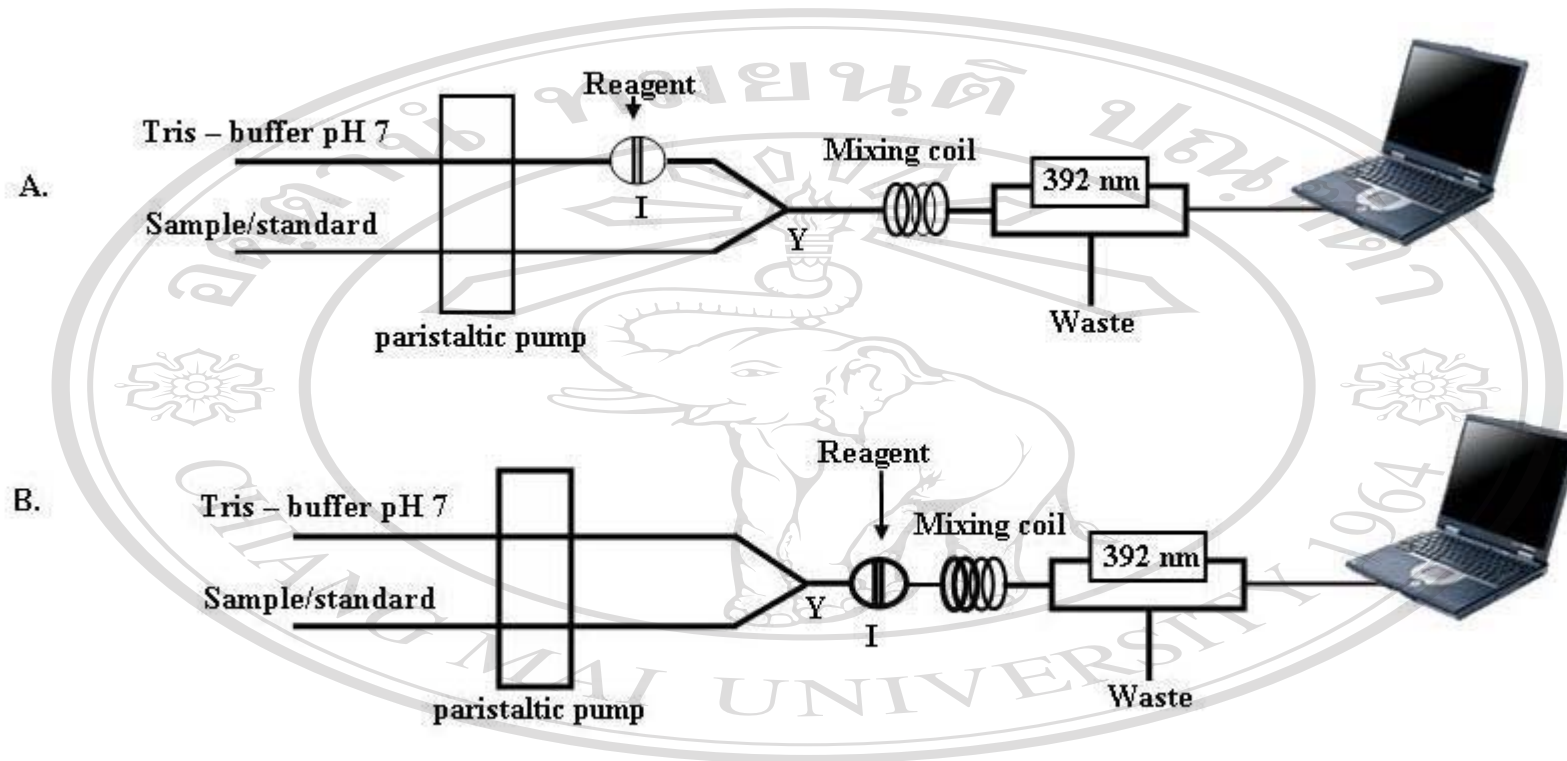
**Figure 3.1** The 2 types of rFI manifolds designed for CTC determination (A) injection of the yttrium (III) as reagent solution into

the buffer stream before merging with the sample/standard solution (B) injection of the reagent solution into the merging stream

of the buffer and sample/standard solution. (Y = Y connector, I = home-made injection valve.

### 3.1.2 Absorption Spectra of CTC and Its Yttrium (III) Complex

The $1 \times 10^{-3}$ mol $l^{-1}$ CTC exhibits its absorption maximum at 355 nm (Figure 3.2A.) in Tris – buffer pH 7.0 medium. CTC reacts with 20 ppm yttrium (III) resulting in a yellow complex in the same medium. The complex presents an absorption maximum of 0.872 at 392 nm (Figure 3.2B.). In the presence of surfactant, $1 \times 10^{-3}$ M CTAB, the yellow color of the complex shows maximum absorbance of 0.974 AU at the same wavelength (Figure 3.2C.).
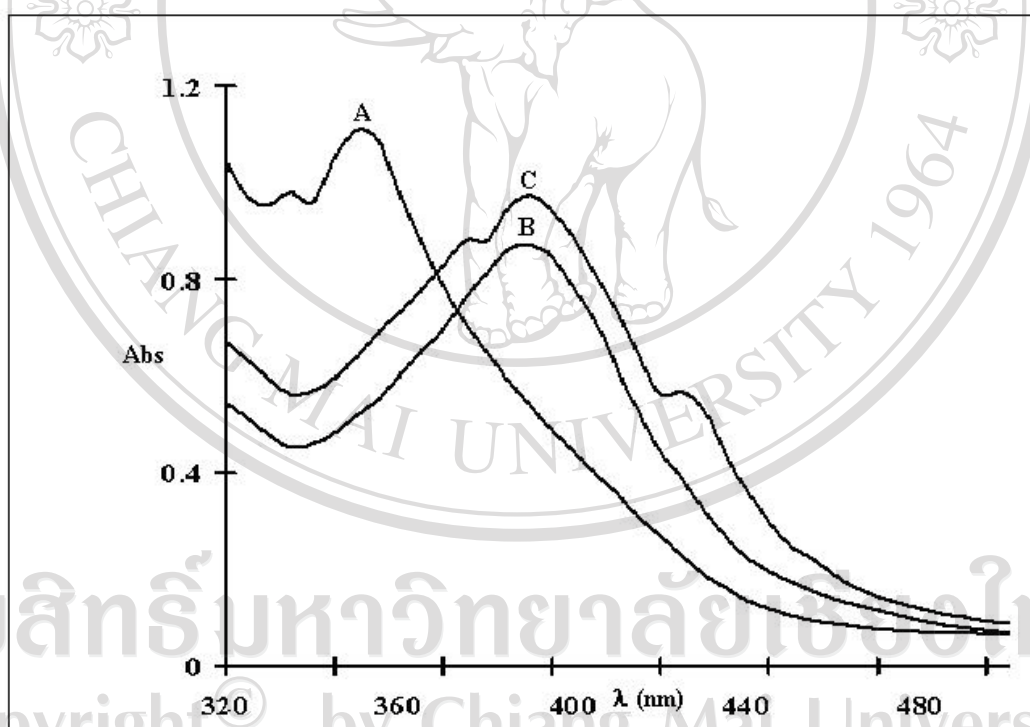
**Figure 3.2** The absorption spectra of CTC (A), CTC-yttrium(III) complex (B) and CTC-yttrium(III) complex in CTAB medium (C)

### 3.1.3 Optimization of Chemical and Physical Variables by Univariate Method

To optimize the experimental conditions, the rFIA manifold in Figure 3.1B was used. The following variables (chosen by random) were fixed with the exception of the variable to be studied; mixing coil length 30 cm with 20 ppm yttrium(III), $1 \times 10^{-3}$ mol $l^{-1}$ CTAB, Tris-buffer pH 7.0, reagent injection volume 100 µl, mixing coil length 30 cm and flow rate 2.0 ml $min^{-1}$ The standard CTC in the range of $1 \times 10^{-5} - 5 \times 10^{-5}$ mol $l^{-1}$.

All optimum values were chosen by judging from the sensitivity of standard curve and reproducibility of the peak heights obtained. Preliminary conditions used were as shown in Table. 3.2

**Table3.2** Preliminary conditions before optimization of the rFI systems

| Variable | Value |
|---|---|
| Yttrium concentration | 20 ppm |
| CTAB concentration | $1 \times 10^{-3}$ mol $l^{-1}$ |
| Tris buffer | pH 7, 0.5 mol $l^{-1}$ |
| Mixing coil length | 30 cm |
| Reagent injection volume | 100 µl |
| Flow rate | 2.0 ml $min^{-1}$ |

### 3.1.3.1 Effect of Wavelength

It is essential to examine the optimum wavelength that give the maximum absorption of the complex of interest including Y(III) – CTC complex to obtained the greatest sensitivity. Therefore effect of wavelength on sensitivity (slope of standard curve) was investigated over the range of 390 - 400 nm to check the performance of the rFI experimental set-up and the wavelength selector. The results obtained are shown in Table 3.3 and Figure 3.3. The sensitivity was found to increase with increasing wavelength and reached the maximum value up to 392 nm which was corresponding to that obtained from the absorption spectra (Fig. 3.2). Further increasing in wavelength the sensitivity decreased gradually. Therefore, 392 nm was chosen throughout the studies. Hence, further measurements were made at 392 nm.

The metal – to – ligand ratio was 1:1[Fig 3.3], which suggested for lanthanide – tetracycline complexes. [237]. The molar absorptivity at 392 nm in Tris-buffer was $4.98 \times 10^4 \, l \, mol^{-1} \, cm^{-1}$ with surfactant medium and without surfactant was $2.86 \times 10^4 \, l \, mol^{-1} \, cm^{-1}$, respectively.
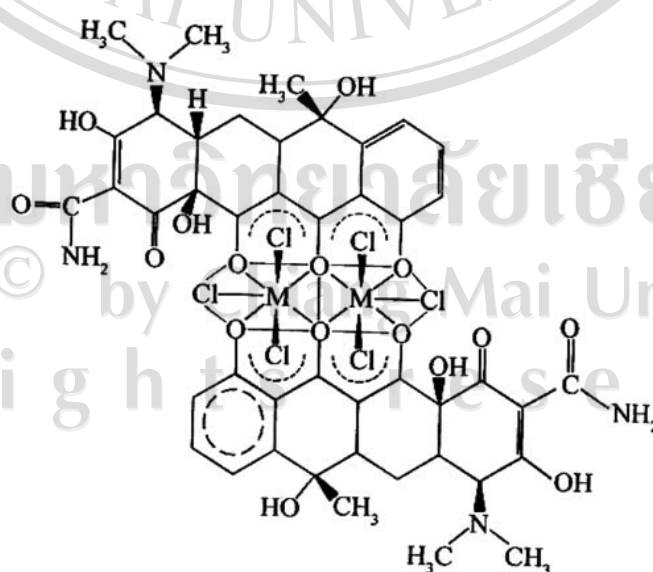


**Figure 3.3** Lanthanide – tetracycline complex [237]

**Table 3.3** Effect of varying wavelengths on analytical signal of CTC from rFI system

| Wave length (nm) | Net signal* (Absorbance unit) obtained from the standard CTC( x 10^-5 mol l^-1) | | | | | y = a(x)+b | R^2 |
|---|---|---|---|---|---|---|---|
| | 1.000 | 2.000 | 3.000 | 4.000 | 5.000 | | |
| 390 | 0.0091 | 0.0121 | 0.0138 | 0.0154 | 0.0174 | y = 202.72x + 0.0075 | 0.9879 |
| 391 | 0.0093 | 0.0129 | 0.0149 | 0.0162 | 0.0178 | y = 204.86x + 0.008 | 0.9594 |
| 392 | 0.0101 | 0.0128 | 0.0148 | 0.0166 | 0.0184 | y = 208.87x + 0.0082 | 0.9923 |
| 393 | 0.0093 | 0.0130 | 0.0150 | 0.0165 | 0.0174 | y = 198.84x + 0.0082 | 0.9372 |
| 394 | 0.0090 | 0.0121 | 0.0134 | 0.0153 | 0.0173 | y = 199.79x + 0.0074 | 0.9876 |
| 395 | 0.0089 | 0.1180 | 0.0131 | 0.0152 | 0.0169 | y = 195.7x + 0.0073 | 0.9903 |
| 396 | 0.0085 | 0.0115 | 0.0129 | 0.0145 | 0.0164 | y = 195.25x + 0.0064 | 0.9895 |
| 397 | 0.0081 | 0.0111 | 0.0124 | 0.0141 | 0.0161 | y = 192.29x + 0.007 | 0.9859 |
| 398 | 0.0073 | 0.0092 | 0.0107 | 0.0132 | 0.0149 | y = 193.23x + 0.0052 | 0.9841 |
| 399 | 0.0071 | 0.0091 | 0.0100 | 0.0128 | 0.0145 | y = 187.32x + 0.005 | 0.9672 |
| 400 | 0.0069 | 0.0087 | 0.0098 | 0.0125 | 0.0142 | y = 186.27x + 0.0047 | 0.9707 |

* Average of three replicate determinations
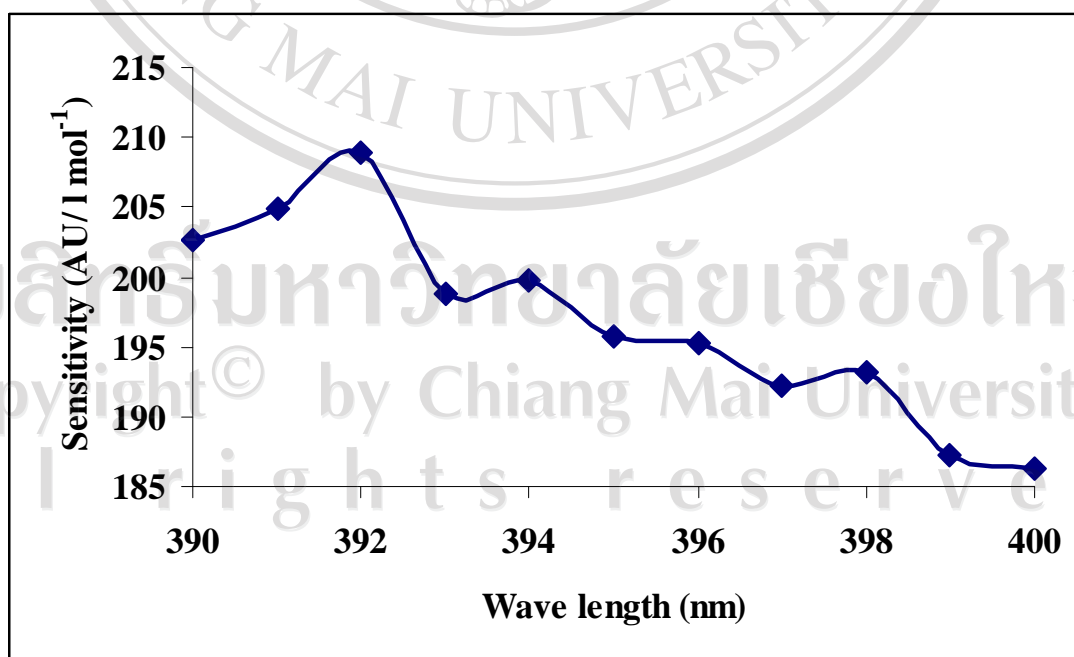


**Figure 3.4** Effect of varying wavelengths on sensitivity for CTC determination

### 3.1.3.2 Effect of pH on the Complex Formation

In general, most complexation reactions are pH dependent. In order to obtain the effective complexation reaction it is necessary to investigate the optimum pH of the reaction media so that the complexation reaction is favored and hence, the sensitivity. The complex formed by the reaction between CTC and yttrium (III) in Tris – buffer medium was studied over the pH range 5.5 – 9.0. The absorption peaks were measured over the above pH range by using Tris – buffer together with a sufficient volume of 1 mol $l^{-1}$ HCl to give the required pH value. The absorption increased when pH values were up to 7.5. Therefore, pH 7.5 was chosen as optimum, because at this pH value the peaks were relatively high with a good sensitivity (defines as slopes of calibration curve) and the linearity of the calibration curve was better than those obtained with other pH values (y = 295.06x + 0.0071, $R^2$ = 0.9991). The results are shown in Table 3.4 and Figure 3.5.

**Table 3.4** Effect of varying pH on analytical signal of CTC from rFI system

| pH | Net signal* (Absorbance unit) obtained from the standard CTC( x $10^{-5}$ mol $l^{-1}$) | | | | | y = a(x)+b | $R^2$ |
|------|--------|--------|--------|--------|--------|----------------------|--------|
|      | 1.000  | 2.000  | 3.000  | 4.000  | 5.000  |                      |        |
| 5.5  | 0.0091 | 0.0126 | 0.0138 | 0.0154 | 0.0175 | y=202.72x + 0.0075   | 0.9890 |
| 6.0  | 0.0092 | 0.0131 | 0.0157 | 0.0179 | 0.0189 | y=244.02x + 0.0076   | 0.9573 |
| 6.5  | 0.0099 | 0.0132 | 0.0164 | 0.0191 | 0.0209 | y= 280.93x + 0.0074  | 0.9882 |
| 7.0  | 0.0100 | 0.0132 | 0.0161 | 0.0189 | 0.0218 | y = 286.85x + 0.0071 | 0.9984 |
| 7.5  | 0.0100 | 0.0128 | 0.0159 | 0.0187 | 0.0213 | y = 295.06x + 0.0071 | 0.9991 |
| 8.0  | 0.0095 | 0.0130 | 0.0161 | 0.0183 | 0.0214 | y = 293.13x + 0.0068 | 0.9956 |
| 8.5  | 0.0098 | 0.0127 | 0.0152 | 0.0176 | 0.0208 | y = 270.92x + 0.0071 | 0.9982 |
| 9.0  | 0.0088 | 0.0120 | 0.0151 | 0.0173 | 0.0201 | y = 280.96x + 0.0062 | 0.9961 |

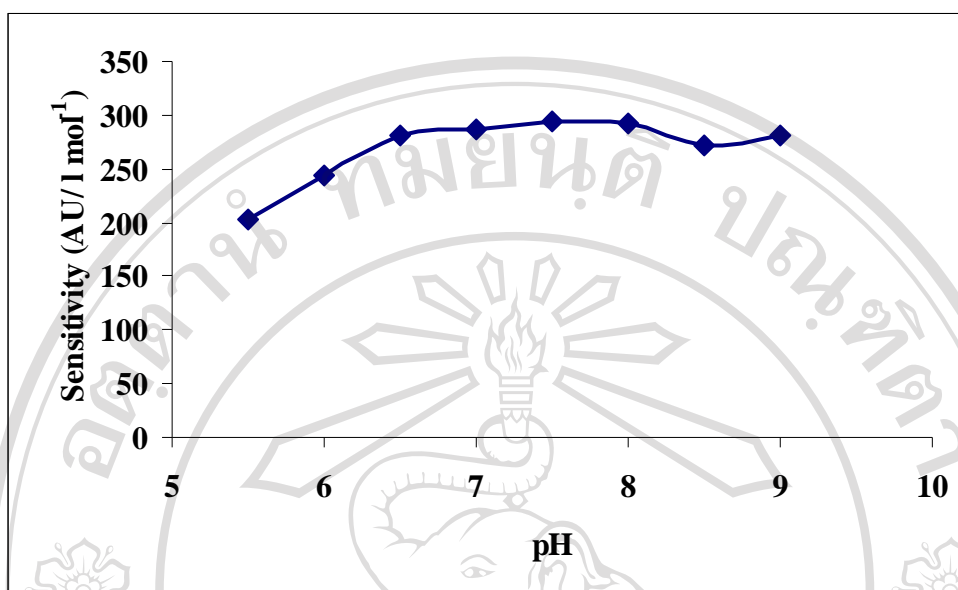\* Average of three replicate determinations

88



**Figure 3.5** Effect of varying pH on sensitivity for CTC determination

### 3.1.3.3 Concentration of Yttrium (III)

Generally, all complexation reactions including complexation between Y(III) and CTC, it is necessary to investigate the optimum concentration of metal ions of interest to achieve the required stoichiometry of the complex (ie., metal to ligand ratio). Then, the effect of various concentrations of yttrium (III) on the absorption peaks of CTC was studied. The CTC concentration range studied (5- 25 ppm) were sufficient for color development. At the higher concentrations of yttrium (III), the slope of standard calibration curve increases. The concentration which provided the largest slope increment was found to be 10 ppm of yttrium (III) concentration. Therefore, it was chosen as optimum yttrium (III) concentration and used through out the experiments. The results were shown in Table 3.5 and Figure 3.6.

**Table 3.5** Effect of yttrium(III) concentration on analytical signal of CTC from rFI

system

| Y(III) ppm | Net signal* (Absorbance unit) obtained from the standard CTC( x $10^{-5}$ mol $l^{-1}$) | | | | | y = a(x)+b | $R^2$ |
|---|---|---|---|---|---|---|---|
| | **1.000** | **2.000** | **3.000** | **4.000** | **5.000** | | |
| 5.0 | 0.0081 | 0.0129 | 0.0145 | 0.0167 | 0.0182 | y = 250.15 + 0.0062 | 0.9727 |
| 10.0 | 0.0087 | 0.0127 | 0.0159 | 0.0183 | 0.0207 | y = 296.31x + 0.0058 | 0.9862 |
| 15.0 | 0.0076 | 0.0128 | 0.0157 | 0.0173 | 0.0191 | y = 288.72 x+ 0.0054 | 0.9792 |
| 20.0 | 0.0075 | 0.0129 | 0.0145 | 0.0173 | 0.0195 | y = 287.05x + 0.0051 | 0.9772 |
| 25.0 | 0.0071 | 0.0128 | 0.0149 | 0.0161 | 0.0182 | y = 272.13x + 0.0052 | 0.9721 |

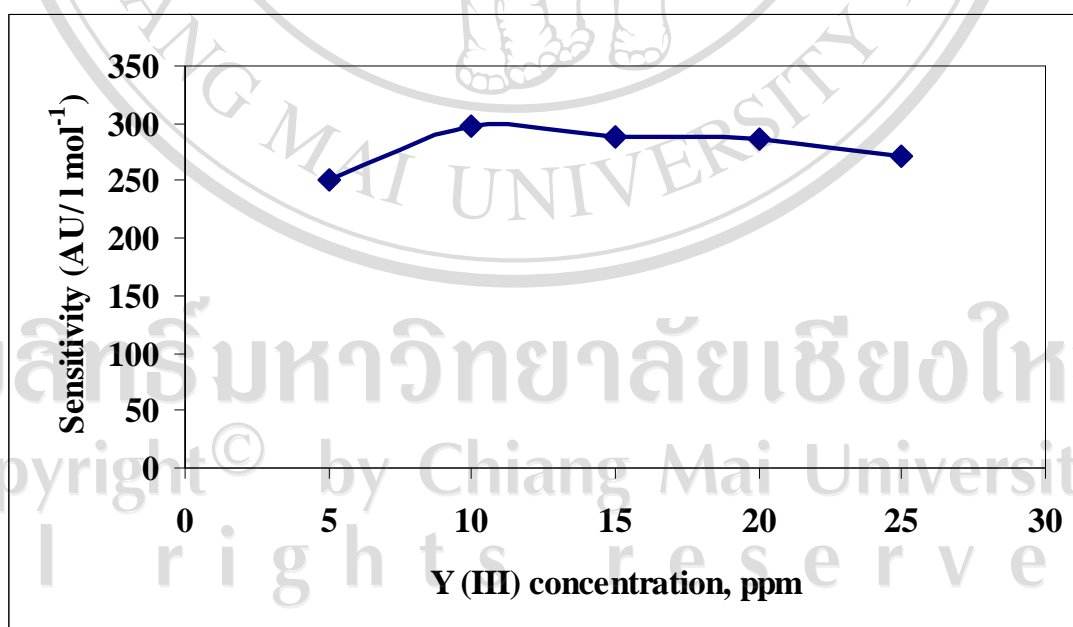\* Average of three replicate determinations



**Figure 3.6** Effect of varying yttrium (III) concentration on sensitivity for CTC

determination

### 3.1.3.4 The Effect Concentration of CTAB

Preliminary experiments pointed out that non-ionic and anionic surfactants could not be added. In fact, the analytical signal was not observed in the presence of these surfactants. Among the different surfactant tested, CTAB was selected because the attainable sensitivity was higher.

In the present work, a cationic surfactant in tris- buffer pH 7.5 was used to obtain the micellar system to enhance the sensitivity of the Y(III) – CTC complex and used as a basic to develop a greener analytical procedure for CTC determination. Therefore, preliminary investigations were carried out by measurement of the peak heights obtained with and without addition of CTAB. It was found that with addition of CTAB surfactant, CTC – Y (III) complex exhibited higher absorption peak than 2 times that obtained in the absence of the surfactant. Concentration of this surfactant plays an important role in the system design. For concentration higher than $8 \times 10^{-4}$ mol $l^{-1}$ (critical micelle concentration), the products formed aggregated themselves. The influence of CTAB concentration on CTC determination was studied over range $2.5 \times 10^{-3} – 1.25 \times 10^{-2}$ mol $l^{-1}$. The response increases with an increase in CTAB concentration, the concentration that was chosen for the best sensitivity and linearity was $5 \times 10^{-3}$ mol $l^{-1}$. The further increment of the CTAB concentration did not recommend because it caused high viscosity and the absorbance did not linearly related with CTC concentration. Results are shown in Table 3.6 and Figure 3.7.

**Table 3.6** Effect of varying CTAB concentration on sensitivity for CTC determination

| [CTAB] mol l$^{-1}$ | Net signal* (Absorbance unit) obtained from the standard CTC( x 10$^{-5}$ mol l$^{-1}$) | | | | | y = a(x)+b | R$^2$ |
|---|---|---|---|---|---|---|---|
| | 1.000 | 2.000 | 3.000 | 4.000 | 5.000 | | |
| 2.5 x 10$^{-3}$ | 0.0064 | 0.0102 | 0.0132 | 0.0167 | 0.0184 | y = 291.03x + 0.004 | 0.9892 |
| 5.0 x 10$^{-3}$ | 0.0075 | 0.0117 | 0.0151 | 0.0189 | 0.0218 | y = 349.75x + 0.0044 | 0.9966 |
| 7.5 x 10$^{-3}$ | 0.0066 | 0.0112 | 0.0146 | 0.0175 | 0.0196 | y = 315.1x + 0.0044 | 0.9740 |
| 10.0 x 10$^{-3}$ | 0.0075 | 0.0116 | 0.0145 | 0.0176 | 0.0191 | y = 284.74x + 0.0055 | 0.9715 |
| 12.5 x 10$^{-3}$ | 0.0082 | 0.0115 | 0.0151 | 0.0168 | 0.0201 | y = 284.54x + 0.0057 | 0.9887 |

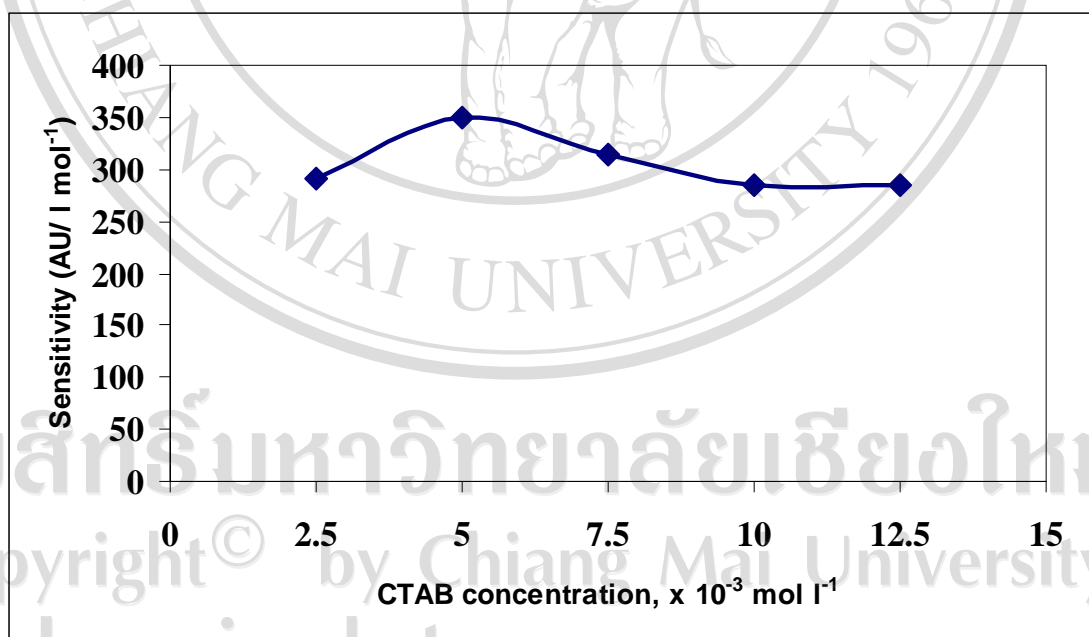\* Average of three replicate determinations



**Figure 3.7** Effect of varying CTAB concentration on sensitivity for CTC determination

### 3.1.3.5 Effect of Mixing Coil Length

The complexing solution between Y(III) and CTC pass through the mixing coil which is the mixing is responsible for ensuring complete reagent mixing resulting in a time delay for development of a reaction between the analyte and reagent. The effect of the mixing coil length was studied by varying from 20 - 80 cm length of PTFE tubing with a diameter of 1.02 mm i.d. It was found that the sensitivity increased with increasing the tubing length up to 50 cm. The further increases in tubing length to 60 cm the sensitivity decrease of rapidly (Table 3.7 and Figure 3.8). Therefore, a 50 cm tubing length was chosen as suitable mixing coil for further experiments.

**Table 3.7** Effect of varying mixing coil length on sensitivity for CTC determination

| Reaction coil length (cm) | Net signal* (Absorbance unit) obtained from the standard CTC( x $10^{-5}$ mol $l^{-1}$) | | | | | y = a(x)+b | $R^2$ |
| | 1.000 | 2.000 | 3.000 | 4.000 | 5.000 | | |
|---|---|---|---|---|---|---|---|
| 20.0 | 0.0046 | 0.0080 | 0.0117 | 0.0140 | 0.0161 | Y = 289.22x + 0.0021 | 0.9898 |
| 30.0 | 0.0082 | 0.0116 | 0.0152 | 0.0188 | 0.0205 | Y = 318x + 0.0053 | 0.9872 |
| 40.0 | 0.0079 | 0.0121 | 0.0149 | 0.0187 | 0.0224 | Y = 356x + 0.0045 | 0.9973 |
| 50.0 | 0.0067 | 0.0118 | 0.0166 | 0.0193 | 0.0229 | Y = 411.86x + 0.0025 | 0.9989 |
| 60.0 | 0.0065 | 0.0112 | 0.0155 | 0.0173 | 0.0210 | Y = 363.65x + 0.0028 | 0.9965 |
| 70.0 | 0.0080 | 0.0115 | 0.0141 | 0.0157 | 0.0188 | Y = 266x + 0.0052 | 0.9971 |
| 80.0 | 0.0072 | 0.0110 | 0.0140 | 0.0152 | 0.0176 | Y = 260x + 0.0048 | 0.9975 |

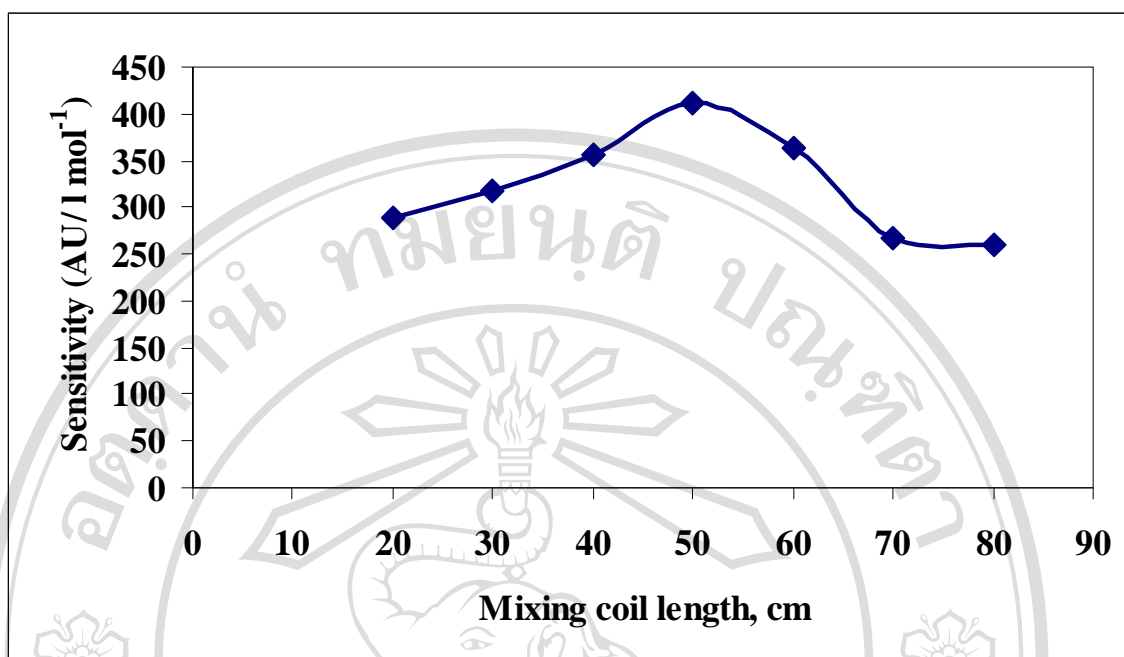* Average of three replicate determinations

**Figure 3.8** Effect of varying mixing coil length on sensitivity for CTC determination

### 3.1.3.6 Effect of Flow Rate

The effect of the flow rate of the carrier and standard/sample was investigated from $1.0 – 3.5$ ml min$^{-1}$. The higher flow rate shortens the reaction times, increases dispersion and a lower the ratio of sample peak to blank peak. Hence the reaction is not allowed to reach completion as indicated by the decrease in absorbance of the complex formed. On the other hand, low flow rates lead to a decrease in sample throughput. A flow rates of 2.5 ml min$^{-1}$ was chosen for both of carrier and standard/sample streams because it provided a dramatically sample throughput (55 h$^{-1}$), the highest sensitivity (defined as slope of calibration curve) of $456 \times 10^5$ AU l mol$^{-1}$ and the better linearity of standard calibration curve ($R^2 = 0.991$, Table 3.8 and Figure 3.9.)

**Table 3.8** Effect of flow rate on sensitivity for CTC determination

| Flow rate ml min$^{-1}$ | Net signal* (Absorbance unit) obtained from the standard CTC( x 10$^{-5}$ mol l$^{-1}$) | | | | | y = a(x)+b | R$^2$ |
|---|---|---|---|---|---|---|---|
| | **1.000** | **2.000** | **3.000** | **4.000** | **5.000** | | |
| 1.0 | 0.0048 | 0.0090 | 0.0112 | 0.0144 | 0.0144 | y= 249.17 + 0.0027 | 0.9891 |
| 1.5 | 0.0075 | 0.0120 | 0.0158 | 0.0190 | 0.0190 | y = 313.83 + 0.0046 | 0.9946 |
| 2.0 | 0.0054 | 0.0121 | 0.0149 | 0.0192 | 0.0192 | y = 383.74x + 0.0023 | 0.9957 |
| 2.5 | 0.0058 | 0.0129 | 0.0167 | 0.0224 | 0.0224 | y = 456.14x + 0.0014 | 0.9991 |
| 3.0 | 0.0069 | 0.0109 | 0.0139 | 0.0175 | 0.0175 | y = 342.46x + 0.0018 | 0.9929 |
| 3.5 | 0.0069 | 0.0111 | 0.0140 | 0.0173 | 0.0173 | y = 328.16x + 0.002 | 0.9912 |

\* Average of three replicate determinations
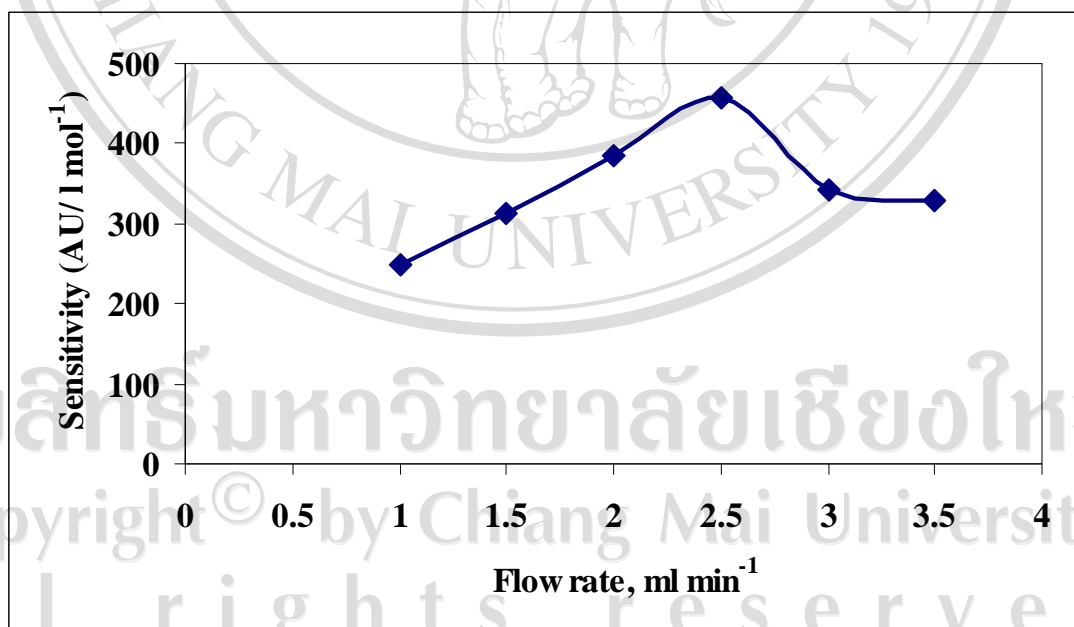


**Figure 3.9** Effect of flow rate on sensitivity for CTC determination

### 3.1.3.7 Effect of Injection Volume

The effect of injection volume was studied by changing the sample loop to give a required injection volume in the range 50 -250 μl in order to find out the optimum injection volume. It was shown that a 200 μl was found to be the optimum injection volume as a compromise between good sensitivity and a sampling frequency of sample per hour. The results are shown in Table 3.9 and Figure 3.10. It was shown that the sensitivity decreased when the injection volume of reagent exceed 200 μl probably owing to the limitation of Beer's law.

**Table 3.9** Effect of injection volume

| Injection volume (μL) | Net signal* (Absorbance unit) obtained from the standard CTC( x $10^{-5}$ mol $l^{-1}$) | | | | | y = a(x)+b | $R^2$ |
|---|---|---|---|---|---|---|---|
| | 1.000 | 2.000 | 3.000 | 4.000 | 5.000 | | |
| 50 | 0.0057 | 0.0095 | 0.0117 | 0.0144 | 0.0159 | y=244.27x + 0.0042 | 0.9865 |
| 100 | 0.0062 | 0.0110 | 0.0135 | 0.0168 | 0.0210 | y = 340.66x + 0.0036 | 0.9939 |
| 150 | 0.0052 | 0.0110 | 0.0136 | 0.0177 | 0.0218 | y =384.34x + 0.0025 | 0.9937 |
| 200 | 0.0055 | 0.0126 | 0.0174 | 0.0210 | 0.0253 | y = 467.37x + 0.0019 | 0.9993 |
| 250 | 0.0071 | 0.0132 | 0.0179 | 0.0209 | 0.0243 | y = 415.6x + 0.004 | 0.9971 |

* Average of three replicate determinations
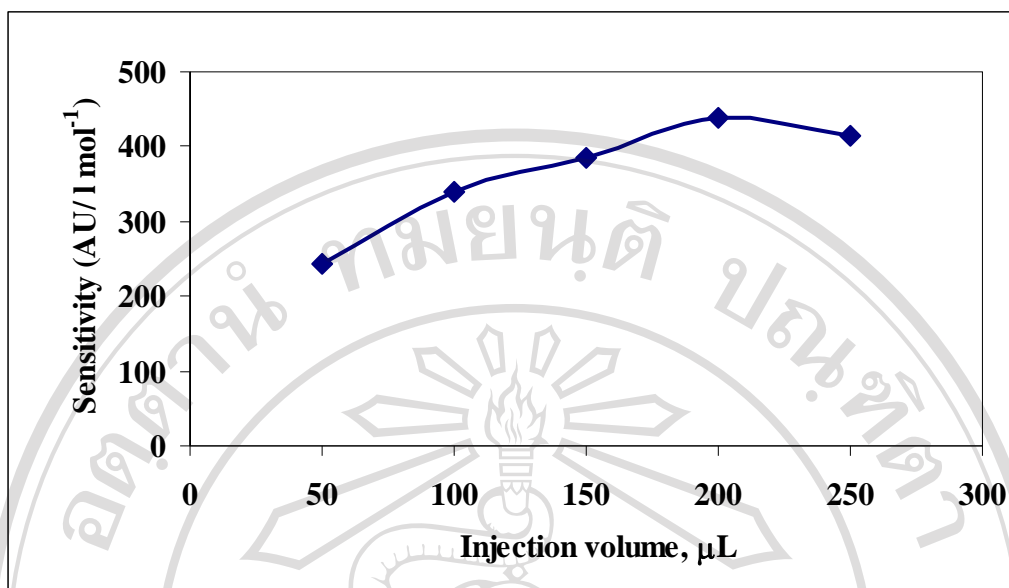
**Figure 3.10** Effect of varying injection volume on sensitivity for CTC determination

### 3.1.3.8 Summary of the Studied Range and Optimized Values

Upon using the univariate method for optimization of the rFI conditions, the following optimum conditions were obtained (Table 3.10).

**Table 3.10** Univariate optimization of chemical and FIA conditions

| Variable | Studied range | Optimized value |
|---|---|---|
| Wavelength (nm) | 330 - 430 | 392 |
| pH of buffer | 5.5 – 9.5 | 7.5 |
| Yttrium(III) concentration ( ppm ) | 5 – 25 | 10.0 |
| CTAB concentration (x $10^{-3}$ mol $l^{-1}$) | 2.5 – 12.5 | 5.0 |
| Mixing coil length (cm) | 20 – 80 | 50.0 |
| Flow rate ( ml min$^{-1}$) | 1.0 – 3.5 | 2.5 |
| Injection volume ( μl) | 50 - 250 | 200 |

### 3.1.4 The Simplex Optimization

In developing a new rFIA method which however involves a large number of independent experiments and may not give an optimum set of experimental conditions. To avoid these problems a simplex method have been utilized in the optimization of the system, and also proved to be efficient techniques. A simplex is a geometric figure in which there are $n + 1$ vertices, where $n$ represents the number of variables [238-239]. However, the initial simplex used in the simplex method is 'hard establishment', that is, prior knowledge has to be obtained about the initial point and step size, making the optimization rather arbitrary. The experimental design can be a powerful tool, but the number of experiments increases dramatically with the increase in number of levels, making the optimization rather complicated. Therefore in this work, the simplex method was used to confirm the optimum conditions, which were obtained by the univariate method. There are five parameters, pH of buffer, yttrium concentration, CTAB concentration, flow rate and mixing coil length, were optimized by the simplex method, while others parameters were optimized by the univariate method. The initial parameters to be optimized were chosen from the optimum conditions obtained by the univariate method; others are those appearing next to the optimum values.

The summarization of the results of the five – variable optimization values were shown in Table 3.11 – 3.15 and Figure 3.11, a total of 18 experiments were performed to decide the optimum conditions. The points 1- 6 represent the first cycle, and the first point is the optimum condition of the univariate technique. The best point attained was point 1 with a slope of 462.57 l mol$^{-1}$; the worst was point 2 with a slope of 227.86 l mol$^{-1}$. Therefore, point 2 was reflected through the centroid of other points

to obtain point 7. An experiment was then performed utilizing the variable setting as the reflected point; a slope of 219.87 l mol$^{-1}$ was obtained. Because this value was not better than the next-to-the-worst point, point 4. Then, by using the experimental setting of variables generated by contraction, a slope of 349.43 l mol$^{-1}$ was obtained, which was not better than the best point. From the complete cycle of simplex method, it was found that the optimum conditions by the simplex optimization are similar to those obtained by the univariate method. The optimum conditions were: yttrium (III) 10 ppm, CTAB 5 x 10$^{-3}$ mol l$^{-1}$, pH 7.5, mixing coil length 50 cm and flow rate 2.5 ml min$^{-1}$.

**Table 3.11** The results of the initial simplex optimization for CTC determination

| Vertex number | Factors | | | | | Response |
|:---:|:---:|:---:|:---:|:---:|:---:|:---:|
| | [Y(III)] ppm | [CTAB] X 10$^{-3}$ mol l$^{-1}$ | pH | Mixing coil, cm | Flow rate mL min$^{-1}$ | |
| 1 | 10.0 | 50.0 | 7.5 | 50.0 | 2.5 | 462.57 |
| 2 | 20.0 | 75.0 | 8.0 | 40.0 | 3.5 | 227.86 |
| 3 | 20.0 | 75.0 | 7.0 | 70.0 | 2.5 | 430.78 |
| 4 | 15.0 | 50.0 | 8.0 | 60.0 | 3.0 | 237.53 |
| 5 | 15.0 | 50.0 | 7.5 | 60.0 | 2.0 | 442.72 |
| 6 | 10.0 | 75.0 | 7.0 | 50.0 | 2.0 | 323.82 |

**Table 3.12** The summarization of the initial simplex optimization

| Simplex No. | Factors | | | | | Response | Rank | Vertex |
| | [Y(III)] | [CTAB] | pH | Mixing | Flow rate | | | |
| 1 -------> 2 | ppm | mmol l⁻¹ | | coil, cm | mL min⁻¹ | | | no. |
|---|---|---|---|---|---|---|---|---|
| | 10.0 | 5.0 | 7.5 | 50.0 | 2.5 | 462.57 | B | 1 |
| | 15.0 | 5.0 | 7.5 | 60.0 | 2.0 | 442.72 | | 5 |
| | 20.0 | 7.5 | 7.0 | 70.0 | 2.5 | 430.78 | | 3 |
| | 10.0 | 7.5 | 7.0 | 50.0 | 2.0 | 323.82 | | 6 |
| | 15.0 | 5.0 | 8.0 | 60.0 | 3.0 | 237.53 | N | 4 |
| Σ | 70.0 | 30.0 | 37.0 | 290.0 | 12.0 | | | |
| P = Σ/k | 14.0 | 6.0 | 7.4 | 58 | 2.4 | | | |
| W | 20.0 | 7.5 | 8.0 | 40.0 | 3.5 | 227.86 | W | 2 |
| (P-W) | -6.0 | -1.5 | -0.6 | 18.0 | -1.1 | | | |
| R=P+(P-W) | 8.0 | 4.5 | 6.8 | 76.0 | 1.3 | 219.87 | R | 7 |
| (P-W)/2 | -3.0 | -0.8 | -0.3 | 9.0 | -0.6 | | | |
| Cw=P-(P-W)/2 | 17.0 | 5.2 | 7.7 | 49.0 | 3.0 | 349.43 | Cw | 8 |
| C$_R$= P+(P-W)/2 | | | | | | | | |
| E = R+(P-W) | | | | | | | | |

**Table 3.13** The summarization of the second simplex optimization

| Simplex No. | Factors | | | | | Response | Rank | Vertex |
| | [Y(III)] | [CTAB] | pH | Mixing | Flow rate | | | |
| 3 -------> 4 | ppm | mol l⁻¹ | | coil, cm | mL min⁻¹ | | | no. |
|---|---|---|---|---|---|---|---|---|
| | 10.0 | 5.0 | 7.5 | 50.0 | 2.5 | 462.57 | B | 1 |
| | 15.0 | 5.0 | 7.5 | 60.0 | 2.0 | 442.72 | | 5 |
| | 20.0 | 7.5 | 7.0 | 70.0 | 2.5 | 430.78 | | 3 |
| | 17.0 | 5.2 | 7.7 | 49.0 | 3.0 | 349.43 | | 8 |
| | 10.0 | 7.5 | 7.0 | 50.0 | 2.0 | 323.82 | N | 6 |
| Σ | 72.0 | 30.2 | 36.7 | 279.0 | 12.0 | | | |
| P = Σ/k | 14.4 | 6.0 | 7.3 | 55.8 | 2.4 | | | |
| W | 15.0 | 5.0 | 8.0 | 60.0 | 3.0 | 237.53 | W | 4 |
| (P-W) | -0.6 | 1.0 | -0.7 | -4.2 | -0.6 | | | |
| R=P+(P-W) | 13.8 | 7.0 | 6.6 | 51.6 | 1.8 | 196.78 | R | 9 |
| (P-W)/2 | -0.3 | 0.5 | -0.4 | -2.1 | -0.3 | | | |
| Cw=P-(P-W)/2 | 14.7 | 5.5 | 7.7 | 57.9 | 2.7 | 426.93 | Cw | 10 |
| CR= P+(P-W)/2 | | | | | | | | |
| E = R+(P-W) | | | | | | | | |

**Table 3.14** The summarization of the third simplex optimization

| Simplex No. | Factors | | | | | Response | Rank | Vertex |
|---|---|---|---|---|---|---|---|---|
| | [Y(III)] | [CTAB] | pH | Mixing | Flow rate | | | |
| 4 -------> 5 | ppm | mol l⁻¹ | | coil, cm | mL min⁻¹ | | | no. |
| | 10.0 | 5.0 | 7.5 | 50.0 | 2.5 | 462.57 | B | 1 |
| | 15.0 | 5.0 | 7.5 | 60.0 | 2.0 | 442.72 | | 5 |
| | 20.0 | 7.5 | 7.0 | 70.0 | 2.5 | 430.78 | | 3 |
| | 14.7 | 5.5 | 7.7 | 57.9 | 2.7 | 426.93 | | 10 |
| | 17.0 | 5.2 | 7.7 | 49.0 | 3.0 | 349.43 | N | 8C |
| Σ | 76.7 | 28.2 | 37.4 | 286.9 | 12.7 | | | |
| P = Σ/k | 15.3 | 5.6 | 7.5 | 57.4 | 2.5 | | | |
| W | 10.0 | 7.5 | 7.0 | 50.0 | 2.0 | 323.82 | W | 6 |
| (P-W) | 5.3 | -1.9 | 0.5 | 7.4 | 0.5 | | | |
| R=P+(P-W) | 20.3 | 3.7 | 8.0 | 64.8 | 3.0 | 329.04 | R | 11 |
| (P-W)/2 | | | | | | | | |
| Cw=P-(P-W)/2 | | | | | | | | |
| CR= P+(P-W)/2 | | | | | | | | |
| E = R+(P-W) | | | | | | | | |
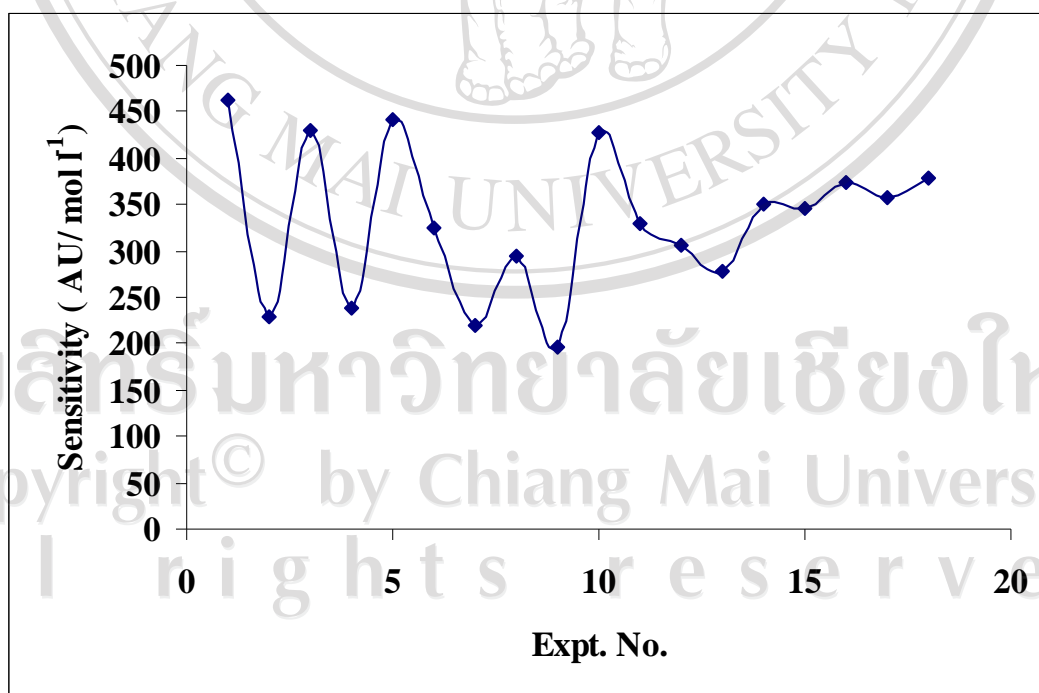


**Figure 3.11** Sensitivity vs. experiment number for simplex method

**Table 3.15** The summarization of all simplex optimization of chemical and FI variables for chlortetracycline determination

| Exp. No.* | Rank | [Y] (ppm) | [CTAB] $(x10^{-3}\ mol\ l^{-1})$ | pH | Mixing coil (cm) | Flow rate $(ml\ min^{-1})$ | Sensitivity |
|---|---|---|---|---|---|---|---|
| 1 | | 10.0 | 5.0 | 7.5 | 50.0 | 2.5 | 462.57 |
| 2 | | 20.0 | 7.5 | 8.0 | 40.0 | 3.5 | 227.86 |
| 3 | | 20.0 | 7.5 | 7.0 | 70.0 | 2.5 | 430.78 |
| 4 | | 15.0 | 5.0 | 8.0 | 60.0 | 3.0 | 237.53 |
| 5 | | 15.0 | 5.0 | 7.5 | 60.0 | 2.0 | 442.72 |
| 6 | | 10.0 | 7.5 | 7.0 | 50.0 | 2.0 | 323.82 |
| 7 | R | 8.0 | 4.5 | 6.8 | 76.0 | 1.3 | 219.87 |
| 8 | $C_W$ | 17.0 | 5.2 | 7.7 | 49.0 | 3.0 | 295.43 |
| 9 | R | 13.8 | 7.0 | 6.6 | 72.0 | 1.3 | 196.78 |
| 10 | $C_W$ | 14.7 | 5.5 | 7.7 | 57.9 | 2.7 | 426.93 |
| 11 | R | 20.3 | 3.7 | 8.0 | 64.8 | 3.0 | 329.04 |
| 12 | R | 10.3 | 7.5 | 7.0 | 50.0 | 3.0 | 305.45 |
| 13 | R | 11.0 | 7.0 | 7.0 | 66.2 | 1.7 | 277.96 |
| 14 | $C_W$ | 15.5 | 5.7 | 7.5 | 53.3 | 2.7 | 351.55 |
| 15 | R | 12.5 | 6.5 | 7.2 | 61.9 | 2.0 | 345.67 |
| 16 | $C_W$ | 14.8 | 5.9 | 7.4 | 55.4 | 2.5 | 374.76 |
| 17 | R | 13.2 | 6.3 | 7.3 | 59.8 | 2.2 | 357.57 |
| 18 | $C_W$ | 14.4 | 6.0 | 7.4 | 56.5 | 2.4 | 378.69 |

### 3.1.5 Analytical Characteristics

#### 3.1.5.1 Calibration Graph and Detection Limit

Using the rFI manifold (Figure 3.1) and the optimum conditions in Table 3.10, the calibration curve was constructed by using series of standard CTC solutions. Results are shown in Table 3.16, Figures 3.12 - 3.13 with the proposed reverse flow injection analysis system for CTC determination. It was found to be a linear plot for the concentration range studied $1.0 \times 10^{-5} - 3.0 \times 10^{-4}$ mol l$^{-1}$, which can be expressed by the regression equation as shown below:

$Y = 3208.5.2X + 0.0137, (R^2 = 0.9993)$

Where $Y$ is the peak height (AU) and $X$ is the CTC concentration in mol l$^{-1}$.

The limit of detection (LOD) was determined from the regression equation with calculated parameters of the intercept of the straight line and three times the standard deviation of the regression time ($3\sigma$) [130]. Based on such a definition, the detection limit of the proposed method was found to be $8.33 \times 10^{-6}$ mol l$^{-1}$ of CTC solution and the limit of quantitation ($10\ \sigma$) was therefore $2.78 \times 10^{-5}$ mol l$^{-1}$.

**Table 3.16** Peak height for calibration curve

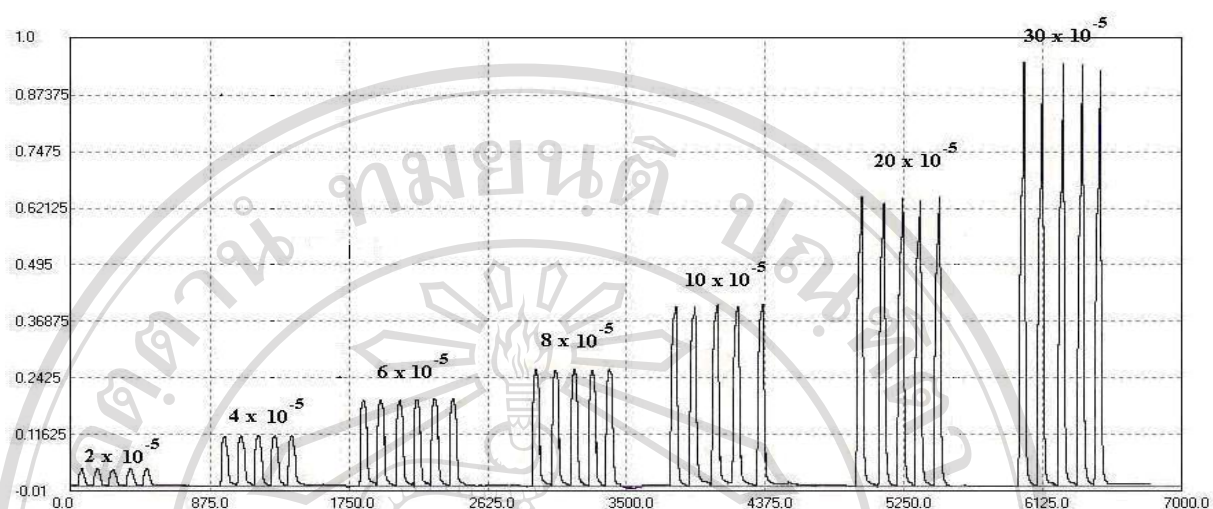| Average concentration of CTC ( x $10^{-5}$ mol l$^{-1}$) ( n = 5 ) | Responses (Absorbance unit) |
|---|---|
| 2.0000 | 0.0712 |
| 4.0000 | 0.1625 |
| 6.0000 | 0.2281 |
| 8.0000 | 0.2845 |
| 10.0000 | 0.3390 |
| 20.0000 | 0.6475 |
| 30.0000 | 0.9756 |

**Figure 3.12** The FIA-gram of standard CTC solutions
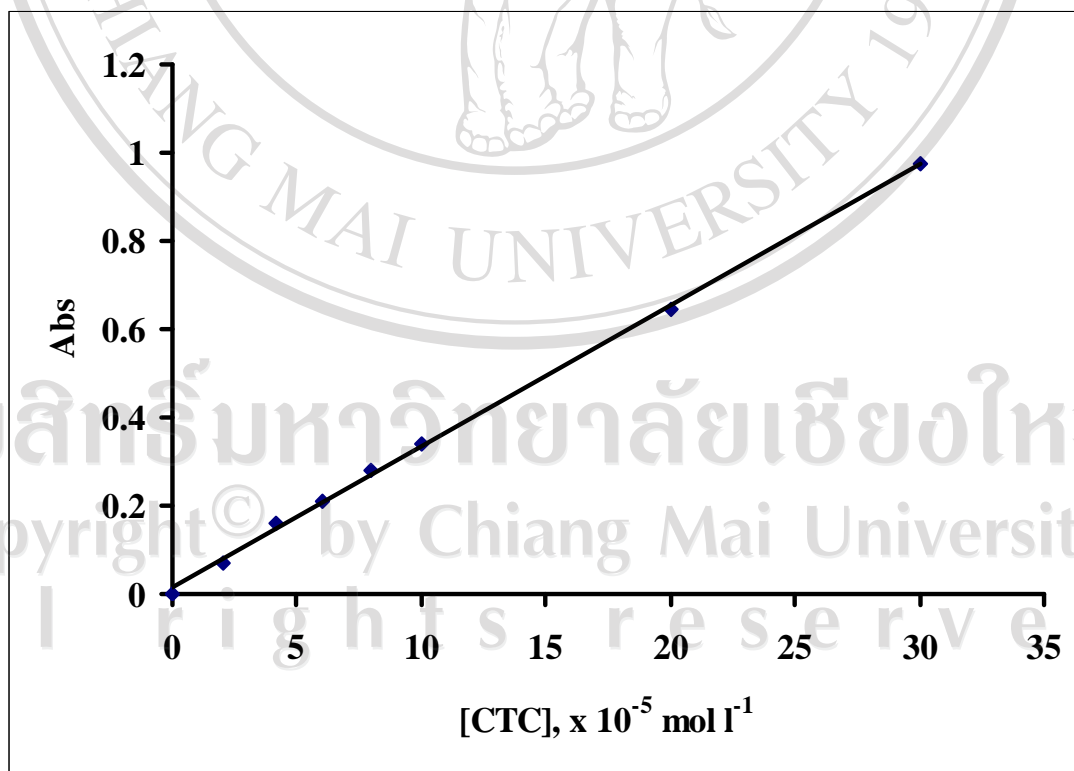


**Figure 3.13** Calibration curve for CTC determination

### 3.1.5.2 Accuracy

The accuracy of the proposed method was verified by standard addition method. The method was examined by determining the recoveries of the added CTC with varying concentrations in sample solution (n=5). The results are presented in Table 3.17. The recoveries were found to be over the range of 99.20 – 101.60 % indicating that the proposed method was accurate.

**Table 3.17** The recoveries of the added CTC with varying concentrations in sample solution (n=5)

| Sample | Added (mg) | Found (mg) | Recovery (%) |
|--------|-----------|-----------|--------------|
| CTC_A | 5 | 5.08 | 101.60 |
| CTC_B | 10 | 9.92 | 99.20 |
| CTC_C | 15 | 14.89 | 99.27 |
| CTC_D | 20 | 20.11 | 100.55 |
| CTC_F | 25 | 24.82 | 99.28 |

### 3.1.5.3 Repeatability and Reproducibility

The repeatability of recommended method was evaluated by using 11 replicates of standard CTC $5.0 \times 10^{-5}$ mol $l^{-1}$ The results are summarized in the Table 3.18. The relative standard deviation was estimated to be 1.12 %. The reproducibility of the method was pursued by determining 11 standard solutions of $5.0 \times 10^{-5}$ mol $l^{-1}$.

**Table 3.18** Repeatability and reproducibility of replicate determination of CTC

| Experiment number | Analytical signal (absorbance unit) | |
|---|---|---|
| | Repeatability | Reproducibility |
| 1 | 0.0223 | 0.0227 |
| 2 | 0.0222 | 0.0231 |
| 3 | 0.0228 | 0.0224 |
| 4 | 0.0225 | 0.0232 |
| 5 | 0.0227 | 0.0221 |
| 6 | 0.0226 | 0.0234 |
| 7 | 0.0229 | 0.0228 |
| 8 | 0.0221 | 0.0222 |
| 9 | 0.0223 | 0.0232 |
| 10 | 0.0225 | 0.0225 |
| 11 | 0.0261 | 0.0224 |
| **Average** | **0.0225** | **0.0227** |
| **Standard deviation** | **0.00025** | **0.00045** |
| **% RSD** | **1.12** | **1.76** |

### 3.1.6 Interference study

Some traditional, common excipients that might be presented in the commercial formulations studied, such as cellulose, fructose, glucose, lactose, maltose, starch and sucrose were examined [Table 3.19]. It was exhibited that the presence of the above mentioned excipients up to 10 to 20 times of the weight ratio to CTC showed no interference effects on CTC determination. Therefore, the developed method is very suitable for determining CTC in commercial pharmaceutical preparations, and hence it is also suitable for quality control in drug industries where is CTC manufactured.

**Table 3.19** Recoveries 2.0 x $10^{-5}$ mol $l^{-1}$ CTC solution in the presence of some excipients ( n=5 )

| Excipient | ratio excipients to CTC (w/w) | Recovery * (%) | Mean (%) | Error (%) |
|---|---|---|---|---|
| **Glucose** | 5 | 100.32, 99.89, 99.67, 100.24, 100.19 | 100.06 | 0.1 |
| | 10 | 99.85, 100.21, 99.88, 100.12, 100.27 | 100.07 | 0.1 |
| | 15 | 100.35, 100.78, 100.86, 100.95,100.54 | 100.70 | 0.7 |
| | 20 | 101.54, 101.76, 102.34, 101.98,101.88 | 101.90 | 1.9 |

* Calculated from average of  5 injections

**Table 3.19** Recoveries 2.0 x $10^{-5}$ mol $l^{-1}$ CTC in solution of some excipients ( n=5 )

(continued)

| Excipient | ratio excipients to CTC (w/w) | Recovery * (%) | Mean (%) | Error (%) |
|---|---|---|---|---|
| Sucrose | 5 | 100.56, 100.78, 100.97, 100.88, 101.07 | 100.85 | 0.9 |
| | 10 | 101.87, 101.96, 102.12, 102.45, 101.93 | 102.07 | 2.1 |
| | 15 | 102.45, 102.76, 103.12, 103.23, 102.65 | 102.84 | 2.8 |
| | 20 | 103.87, 104.67, 104.98, 105.02, 104.76 | 104.66 | 4.7 |
| Starch | 5 | 100.95, 101.23, 100.79, 101.45, 101.33 | 101.15 | 0.2 |
| | 10 | 102.35, 101.56, 101.76, 102.03, 102.12 | 101.96 | 1.0 |
| | 15 | 103.45, 103.79, 104.15, 103.98, 104.45 | 103.96 | 4.0 |
| | 20 | 104.76, 105.21, 105.56, 104.25, 104.78 | 104.91 | 4.9 |

**Table 3.19** Recoveries 2.0 x $10^{-5}$ mol $l^{-1}$ CTC in solution of some excipients ( n=5 )

(continued)

| Excipient | ratio excipients to CTC (w/w) | Recovery * (%) | Mean (%) | Error (%) |
|---|---|---|---|---|
| Cellulose | 5 | 99.45, 104.56, 107.43, 99.23, 101.54 | 102.44 | 2.4 |
| | 10 | 104.67, 101.45, 99.23, 99.45, 105.69 | 102.64 | 2.6 |
| | 15 | 99.62, 105.67, 104.15, 104.56, 101.35 | 103.07 | 3.1 |
| | 20 | 104.78, 108.45, 101.42, 107.54, 101.74 | 104.79 | 4.8 |
| Maltose | 5 | 98.54, 99.23, 98.67, 97.45, 98.35 | 98.45 | -1.6 |
| | 10 | 98.56, 99.55, 98.76, 99.23, 98.13 | 98.85 | -1.2 |
| | 15 | 100.34, 99.96, 100.15, 100.05, 101.84 | 100.47 | 0.5 |
| | 20 | 101.45, 99.87, 100.57, 101.65, 101.35 | 100.98 | 1.0 |
| Fructose | 5 | 100.55, 99.97, 100.86, 101.58, 101.57 | 100.91 | 0.9 |
| | 10 | 102.78, 103.68, 103.44, 102.87, 102.65 | 103.08 | 3.1 |
| | 15 | 104.67, 104.83, 105.15, 105.27, 104.91 | 104.91 | 4.9 |
| | 20 | 106.57, 107.64, 106.33, 107.04, 106.45 | 106.81 | 6.8 |

**Table 3.19** Recoveries 2.0 x $10^{-5}$ mol $l^{-1}$ CTC in solution of some excipients ( n=5 )
(continued)

| Excipient | excipients to CTC (w/w) | Recovery * (%) | Mean (%) | Error (%) |
|---|---|---|---|---|
| Lactose | 5 | 101.56, 102.35, 101.67, 102.55, 102.61 | 102.48 | 2.5 |
| | 10 | 104.59, 104.38, 105.05, 104.77, 104.52 | 104.66 | 4.7 |
| | 15 | 106.97, 106.85, 107.22, 107.15, 107.32 | 107.10 | 7.1 |
| | 20 | 108.67, 108.43, 107.75, 108.45, 107.58 | 108.18 | 8.2 |

* Calculated from average of 5 injections

### 3.1.7 Determination of CTC in Pharmaceutical Preparations

The present FIA manifold was therefore applied to the determination of CTC in

pharmaceutical formulations available in Thailand. The results obtained are presented

in Table 3.20. When compared the results with those obtained by the conventional

spectrophotometric method [240]. It was shown that the results obtained by both

methods were not different signigicantly. The Student's *t*-Test values indicated less

than the theoretical values at a confident level of 95%.

**Table 3.20** Comparative determination CTC in commercial pharmaceutical preparations by the proposed and reference procedures

| Sample | Mean content ± SD* (mg) | | Calculated $t$- test value[††] | % labeled amount |
|---|---|---|---|---|
| | FI method | Conventional spectrophotometric Method[†] | | |
| CTC 1 | 250.8 ± 0.42 | 251.1 ± 0.21 | 1.03 | 100.03 |
| CTC 2 | 251.1 ± 0.75 | 250.2 ± 0.95 | 0.95 | 101.07 |
| CTC 3 | 250.7 ± 1.18 | 251.3 ± 0.60 | 1.13 | 100.03 |
| CTC 4 | 251.2 ± 0.82 | 250.6 ± 0.75 | 1.15 | 101.08 |
| CTC 5 | 250.8 ± 0.63 | 251.4 ± 0.97 | 1.21 | 100.03 |
| CTC 6 | 250.81 ± 0.42 | 250.85 ± 0.33 | 0.41 | 100.34 |
| CTC 7 | 250.98 ± 0.35 | 250.57 ± 0.87 | 0.19 | 100.38 |
| CTC 8 | 250.01 ± 0.51 | 250.28 ± 0.78 | 0.44 | 100.11 |
| CTC 9 | 250.70 ± 0.48 | 250.74 ± 0.67 | 0.46 | 100.30 |
| CTC 10 | 250.56 ± 0.48 | 250.17 ± 1.00 | 0.22 | 100.22 |

*The claimed value for all samples was 250 mg per capsule and $n = 5$,
[†] Ref. 240.
[††] $t$ theoretical = 2.31 , $n = 5$

## 3.2 Sequential Injection Analysis Determination of Zinc (II) in Pharmaceutical Preparations

The enhancement (sensitization) of the color reactions of metal ions with chelating dyes by the presence of surfactants provides an inexpensive alternative means to spectrometric methods, for meeting the present demands for determination of ever lower concentrations of elements. Choice of surfactant (anionic, cationic or non – ionic surfactants) depends on the nature of the metal complexes concerned. The colored complexes formed in micellar media are characterized by high molar absorptivities (often greater than $10^5$ $1$ $mol^{-1}$ $cm^{-1}$) and high stability over a wide pH range, and usually by a large bathochromic shift caused by addition of surfactants to the binary complex formed in water. Knowledge of the fundamental aspects of these surfactants sensitized reaction should be invaluable in the understanding and design of new analytical methods. Unfortunately, very little attention has been paid so far to the study of the mechanism and nature of such micellar effects.

Currently, surfactant systems used in development of many spectrophotometric method for determining micro amounts of metal ions anion, biological compounds, drugs and pesticides [241] have been increasingly employed and published in a number of articles [242 – 254]. Table 3.21 briefly reviews spectrophotometric determination of zinc by using the chromatic reagents in micellar media.

This study proposes the use of an SIA method for the spectrophotometric determination of zinc(II), using PAN as chromogenic reagent. To avoid the solvent extraction procedure, it was found that Zn(II) – PAN complex can be solubilized by a non – ionic surfactant. Because of the high sensitivity inherent in the use of PAN, it was decided to investigate solubilization of Zn(II) -PAN complex as the basis to

develop a novel method for zinc(II) determination with a non- ionic surfactant. The pink colored Zn(II) –PAN complex in micellar media is detected. The proposed method has been successfully applied to the determination of zinc(II) in pharmaceutical preparations available in Chiang Mai.

Preliminary experiments revealed that suitable conditions for dissolving Zn – PAN complex in aqueous solution could be achieved by adding some non – ionic surfactants such as Tween – 80, Triton X – 100, poly(vinylalcohol) were successively added at different concentrations (0.1 – 1.0 % v/v) into the reaction medium. Preliminary experiments pointed out that cationic surfactants could not be used for this purpose. In fact, the analytical signal was not observed in the presence of cetyltrimethylammonium or cetrypriridinium chloride, in view of the hydration caused by the ionic group [255] that reduced the molecular forces impairing the dissolution, thus the establishment of the organized medium. Cationic surfactants were then not investigated further. Among the different non – ionic surfactants tested, Triton X – 100 was selected because the attainable sensitivity was the highest.

### 3.2.1 Optimization of Chemical and Physical Variable

Using the proposed SIA manifold as shown in Figure 2.1 for the spectrophotometric determination of zinc(II), using PAN as chromogenic reagent. To avoid the extraction procedure, it was found that Zn(II) – PAN complex can be solubilized by a non – ionic surfactant, Triton X – 100. Because of the high sensitivity inherent in the use of PAN, it was decided to investigate solubilization of Zn(II) -PAN complex as the basis to develop a novel method for zinc determination with Triton X – 100. The pink colored Zn(II)–PAN complex in micellar media is detected

spectrophotometrically at 553 nm. NaF and KCN were used as masking agents for Fe(III), Mn(II) and Cu (II). The proposed method has been successfully applied to the determination of zinc (II) in pharmaceutical preparations.

To optimize the conditions, the SIA manifold in Fig.2.2 was used. Initially, the following parameters were kept constant (chosen by random). Preliminary conditions used were shown in Table 3.22.

**Table 3.21** The spectrophotometric determination of zinc(II) by complexing with various chromogenic reagents in micellar media

| reagent | surfactant | $\lambda_{max}$ (nm) | pH | $\varepsilon$ x $10^4$ l mol$^{-1}$ cm$^{-1}$) | Ref |
|---|---|---|---|---|---|
| Chrome azural S | Zephiramine | 510 | - | 9.5 | [242] |
| Methylthymol blue | CPC | 600 | - | 1.57 | [243] |
| stylbaso | CPC | 576 | 8.0 - 10 | 5.6 | [244] |
| Pyrocatechol violet | CPC | 690 | 9.0 | 1.3 | [245] |
| 3,5-diBr-PADMAP[a] | - | 610 | - | 12.6 | [246] |
| 3,5-diBr-PADAP[b] | - | 570 | - | 13.0 | [247] |
| Dithizone | SDS | 538 | 9.0 | 6.6 | [248] |
| Xylenol orange | CPC | 580 | 5.1 | 1.1 | [249] |
| Cadion 2B | Triton X-100 | 524 | 9.2 | 10.0 | [250] |
| Hydrazidazol | Triton X-100 | 640 | 7.5 | 2.7 | [251] |
| 1-(2- Thiazolylazo)2- naphthol | Triton X-100 | 582 | 6.2-8.0 | 4.5 | [252] |
| 4-(2-Arsonophenylazo) salycilic acid | - | 525 | 6.0 | 1.36 | [253] |
| 1-(o-carboxyphenyl)-3-acetyl-5-m-tolylformazan | CPC | 599 | 6.5 | 13.7 | [254] |

**Table3.22** Preliminary conditions before optimization of the SI systems

| parameters | value |
|---|---|
| pH of carbonate buffer solution | 7.0 |
| Flow rate | |
| - Flow rate of aspiration of sample and reagents | 30 µl s$^{-1}$ |
| - Flow rate of sending sample to detector | 30 µl s$^{-1}$ |
| Buffer aspiration volumes | 50 µl |
| Triton X - 100 aspiration volumes | 50 µl |
| Sample aspiration volumes | 50 µl |
| PAN reagent aspiration volumes | 50 µl |
| PAN concentration | 1 X 10$^{-5}$ mol l$^{-1}$ |
| Triton X – 100 concentration | 0.5 % v/v |
| Reaction coil diameter | 0.7 mm. |
| Wavelength | 553 nm |

### 3.2.1.1 Spectral Characteristics

The absorption spectra of PAN and its zinc(II) complex in the presence of

Triton X – 100 were scanned over a range of 350 – 700 nm and shown in Figure 3.14.

In the presence of surfactant, the pink color of zinc(II) complex formed at pH 9.0

showing maximum absorbance of 0.368 at 553 nm (spectrum B) , the blank (PAN –

Triton X -100) shows the maximum absorbance of 0.498 at 474 nm (spectrum A).

Hence, further measurements were made at 553 nm because at this wavelength the

bank signal was found to be minimized.
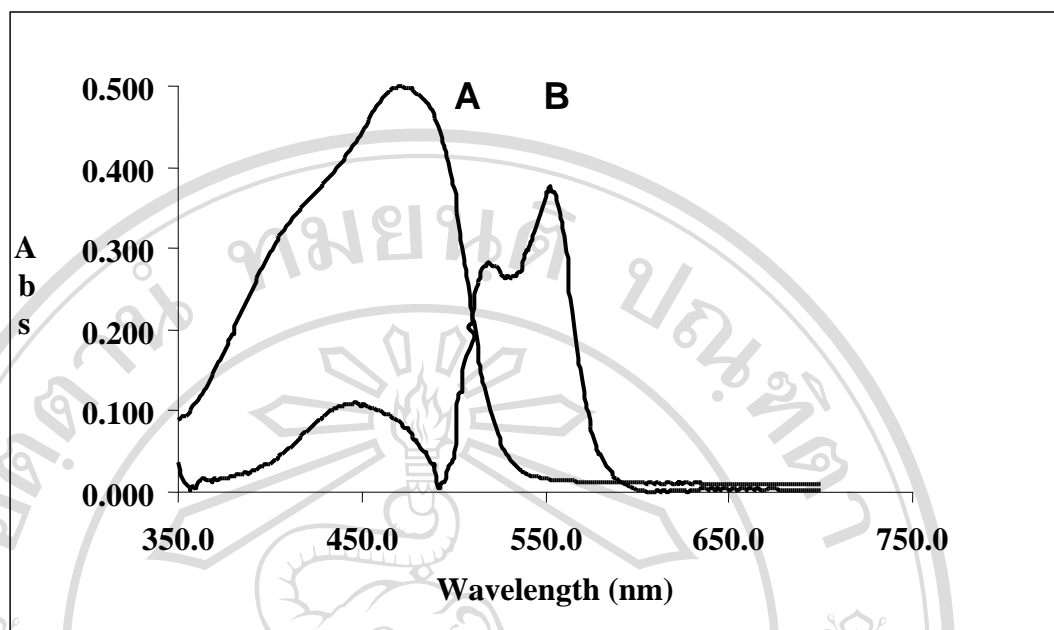
**Figure 3.14** Absorption spectra of zinc complex and its reagent blank curve. (A) PAN – Triton X – 100, (B) zinc– PAN – Triton X –100. The concentration of zinc(II) = 5 µg ml$^{-1}$, PAN = $1.0 \times 10^{-4}$ mol l$^{-1}$, and Triton X – 100 = 1%, respectively ; in carbonate buffer solution pH = 9.0

### 3.2.1.2 Effect of Wavelength

The effect of wavelength on peak height and precision was investigated over the range of 550 - 560 nm to check the performance of the SIA experimental set-up and the wavelength selector. The results obtained are shown in Table 3.23 and Figure 3.15. The peak height and precision were found to increase with increasing wavelength and reached the maximum value up to 553 nm. Further increasing in wavelength the peak height decreased gradually. Therefore, 553 nm was chosen throughout the studies. The optimum wavelength by the proposed method is found to be the same as that found in the absorption spectrum as shown in Figure 3.14.

**Table 3.23** The influence of wavelength on response and precision

| Wavelength (nm) | Peak height (mV) | | | | | %RSD |
|---|---|---|---|---|---|---|
| | **1** | **2** | **3** | **4** | **Mean** | |
| 550 | 3.96 | 3.92 | 3.98 | 3.91 | 3.94 | 0.73 |
| 551 | 4.15 | 4.12 | 4.10 | 4.14 | 4.13 | 0.47 |
| 552 | 4.20 | 4.18 | 4.17 | 4.15 | 4.18 | 0.43 |
| 553 | 4.22 | 4.19 | 4.19 | 4.23 | 4.21 | 0.42 |
| 554 | 4.19 | 4.17 | 4.19 | 4.24 | 4.20 | 0.62 |
| 555 | 4.18 | 4.16 | 4.19 | 4.21 | 4.19 | 0.43 |
| 556 | 4.09 | 4.11 | 4.07 | 4.11 | 4.10 | 0.40 |
| 557 | 4.05 | 4.03 | 4.01 | 4.07 | 4.04 | 0.55 |
| 558 | 4.01 | 3.96 | 3.97 | 3.95 | 3.97 | 0.57 |
| 559 | 3.87 | 3.85 | 3.87 | 3.84 | 3.86 | 0.33 |
| 560 | 3.77 | 3.74 | 3.76 | 3.72 | 3.75 | 0.51 |
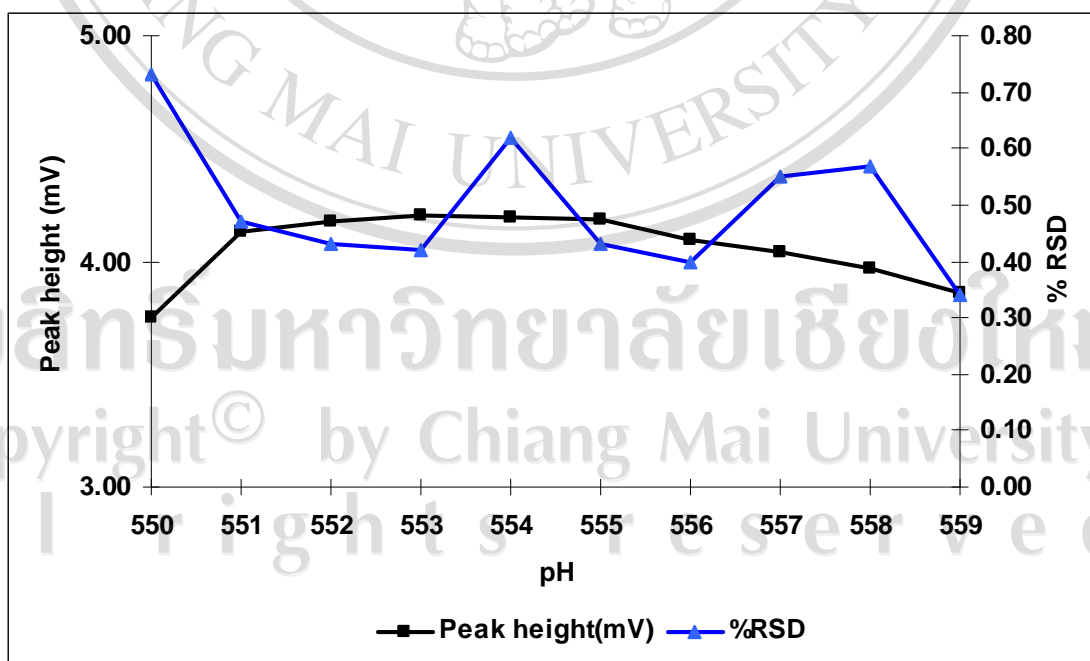


**Figure 3.15** Influence of wavelength on response and precision

### 3.2.1.3 Optimum Conditions for the Reaction

The parameters that influence the sensitivity, accuracy and reproducibility of the proposed method for determining the analyte of interest, zinc (II) were studied in order to establish the optimum working configurations. In all cases both the mean relative peak height (for n = 4 repetitive determinations) and the relative standard deviation were used as a criteria for establishing the most appropriate parameter. All the optimization steps were carried out with a chosen zinc concentration of 0.5 µg ml$^{-1}$, with the fixed concentrations of 0.5 %v/v Triton X -100, and $1 \times 10^{-5}$ mol l$^{-1}$ PAN.

#### 3.2.1.3.1 Effect of pH

The influences of pH on the absorbance (as peak height in mV) of zinc(II) complex was studied over the pH range 5.5 - 10 at 553 nm (Figure 3.16). The pH was adjusted to the desired values using carbonate buffer. It was found that, the chelate was completed at pH values higher than 7, the peak height became significant when the pH exceeded about 10. A pH 9.5 was chosen as the optimum for these reasons and because the carbonate – bicarbonate buffer system has maximum buffer capacity at this pH. The effect of carbonate buffer concentration was studied over the range 0.01-0.1 mol l$^{-1}$. The results demonstrate that it slightly increases in the range 0.01 – 0.05 mol l$^{-1}$. Further increment of the buffer concentrations the peak heights remain constant over the concentration range 0.05 – 0.1 mol l$^{-1}$. Thus, the concentration 0.05 mol l$^{-1}$ of carbonate buffer was chosen for subsequent experiments (Table 3.24).

**Table 3.24** Influence of pH on peak heights and precision

| pH | Peak height (mV) | | | | | %RSD |
|---|---|---|---|---|---|---|
| | **1** | **2** | **3** | **4** | **Mean** | |
| 5.5 | 1.28 | 1.31 | 1.29 | 1.32 | 1.30 | 1.22 |
| 6.0 | 1.45 | 1.44 | 1.47 | 1.49 | 1.47 | 1.31 |
| 6.5 | 1.49 | 1.54 | 1.52 | 1.52 | 1.52 | 1.18 |
| 7.0 | 2.55 | 2.53 | 2.53 | 2.49 | 2.53 | 0.86 |
| 7.5 | 3.27 | 3.29 | 3.25 | 3.25 | 3.27 | 0.51 |
| 8.0 | 3.74 | 3.72 | 3.77 | 3.75 | 3.75 | 0.48 |
| 8.5 | 3.94 | 3.94 | 4.01 | 3.98 | 3.97 | 0.74 |
| 9.0 | 4.05 | 4.01 | 3.98 | 4.05 | 4.02 | 0.73 |
| 9.5 | 4.20 | 4.21 | 4.18 | 4.23 | 4.15 | 0.43 |
| 10.0 | 4.17 | 4.15 | 4.12 | 4.17 | 4.20 | 0.49 |
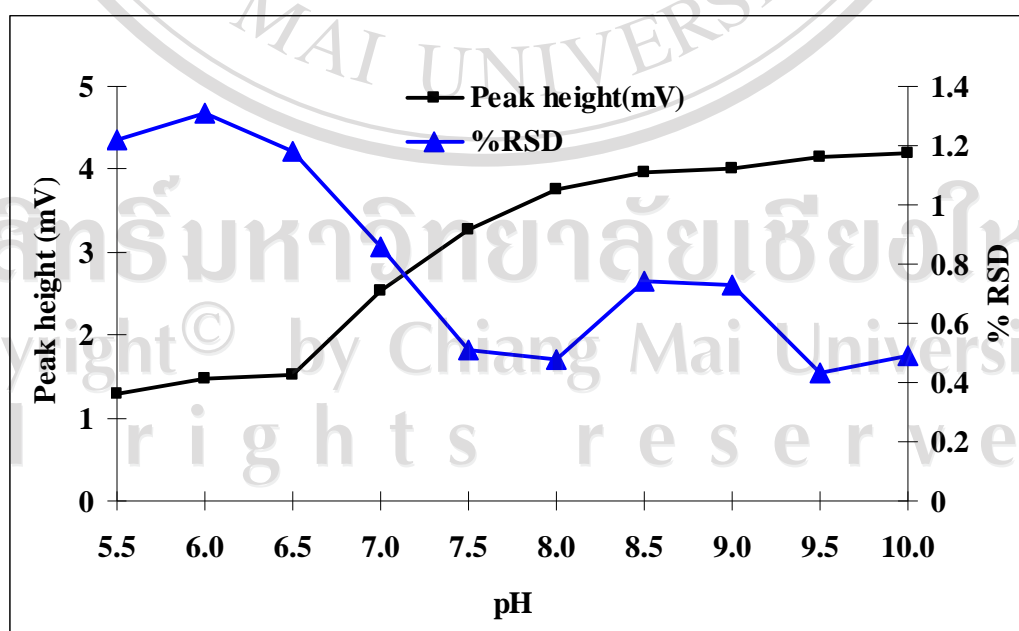


**Figure 3.16** Influence of pH on response and precision

### 3.2.1.3.2 Aspiration Order of Reagents and Sample

In reactions involving multiple zone penetrations, it is essential to examine the aspiration order of reagents and sample [256]. Several aspiration orders have been designed using the SI set – up shown in Table 3.25. It was found that, the order of the aspiration of the sample and reagent was proved to be critical. The appropriate order for aspiration of reagents and sample are as follows: combined masking agent – buffer solution, Triton X- 100, sample and PAN reagent, respectively because it provides the highest signal (mean peak height of 5.54 mV, n=4)  with the best repeatability (% RSD = 0.24) and hence this aspiration order is chosen for subsequent measurements (Figure 3.17).

Where;

(a) = Sam./Triton.[a] – masking buffer[b] – PAN

(b) = masking buffer – PAN – Sam./Triton.[a]

(c) = masking buffer – Sam./Triton[a].-PAN

(d) = masking buffer – Sam.[c] – Triton.[d] – PAN

(e) = masking buffer – Triton.[d] – Sam.[c] – PAN

(f) = masking buffer – Triton.[d] – PAN – Sam.[c]

(g) = Sam.[c] – masking buffer – Triton.[c] – PAN

(h) = Sam.[c] - Triton.- masking buffer – PAN

(i) = Sam.[c] – masking – PAN – Triton.

[a] Sample ( Zn(II) 1 ppm) in 0.5 % v/v Triton X – 100

[b] Combined masking agent and buffer solution pH 9.5

[c] Sample ( Zn(II) 0.5 µg ml$^{-1}$)

[d] 0.5 % v/v Triton X  - 100

### 3.2.1.3.3 Effect of Flow Rate

In any flow – based analysis procedure the response is dependent on the reagents and sample flow rates and thus it is necessary to optimize them to achieve the greatest sensitivity, reproducibility, sample throughput etc.

### a) Optimization of Sample and Reagent Flow Rates

It was obvious that the flow rates of aspiration of sample and reagent were significant with the peak height. The reagent and sample flow rates were investigated from 15 – 50 µl s$^{-1}$ at every 5 µl s$^{-1}$ interval while the flow rate of delivering sample to detector was kept constant at 50 µl s$^{-1}$. As the flow rate increases the peak height increases up to 35 µl s$^{-1}$, whereas after that it tends to level off. The flow rate chosen for yielding the best results was 25 µl s$^{-1}$ (best precision) and it was best for Triton X – 100 aspiration because the faster aspirate, the bubble can occur in the line of stream. The results were shown in Tables 3.26 - 3.27 and Figures 3.18 - 3.19 for sample and reagent respectively.

**Table3.25** Influence of aspiration order of reagent and sample

| Aspiration order | Peak height (mV) | | | | | %RSD |
|---|---|---|---|---|---|---|
| | 1 | 2 | 3 | 4 | Mean | |
| (a) | 3.33 | 3.39 | 3.36 | 3.42 | 3.38 | 0.99 |
| (b) | 3.56 | 3.52 | 3.54 | 3.52 | 3.53 | 0.37 |
| (c) | 3.71 | 3.74 | 3.74 | 3.69 | 3.72 | 0.57 |
| (d) | 4.98 | 5.02 | 5.04 | 5.05 | 5.02 | 0.53 |
| (e) | 5.51 | 5.52 | 5.54 | 5.56 | 5.53 | 0.35 |
| (f) | 4.83 | 4.86 | 4.81 | 4.85 | 4.83 | 0.40 |
| (g) | 4.76 | 4.80 | 4.73 | 4.72 | 4.75 | 0.65 |
| (h) | 4.57 | 4.59 | 4.58 | 4.51 | 4.56 | 0.68 |
| (i) | 3.90 | 3.86 | 3.94 | 3.96 | 3.92 | 0.98 |
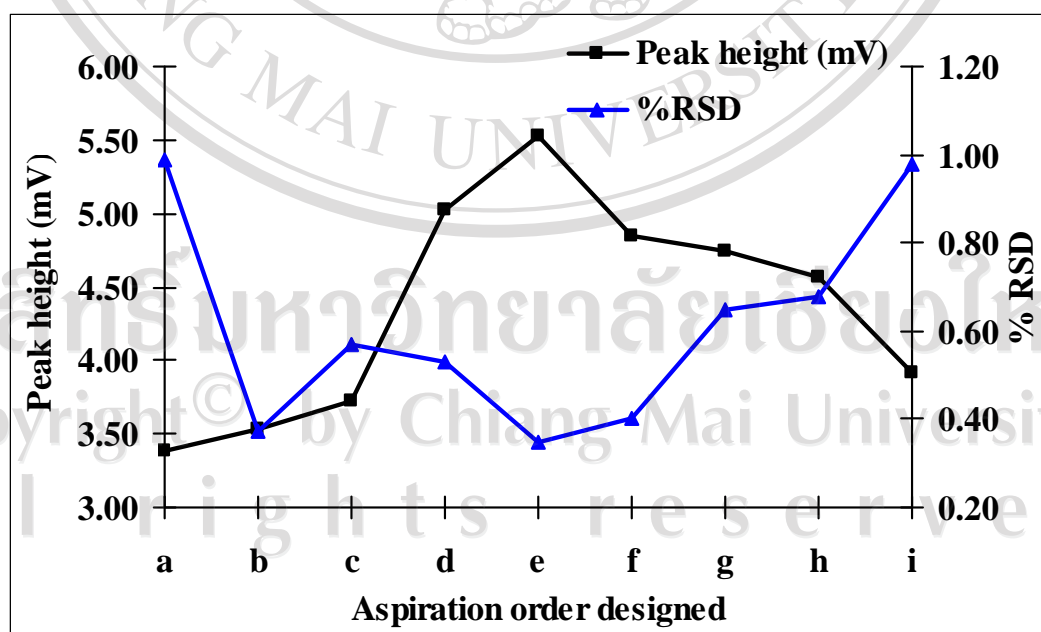


**Figure 3.17** Influence of the aspiration order designed on the response and precision

**Table3.26** Influence of flow rate of aspiration of sample on response and precision

| Flow rate | Peak height (mV) | | | | | %RSD |
|---|---|---|---|---|---|---|
| ($\mu$l s$^{-1}$) | 1 | 2 | 3 | 4 | Mean | |
| 15 | 3.56 | 3.60 | 3.63 | 3.52 | 3.58 | 1.16 |
| 20 | 3.78 | 3.82 | 3.85 | 3.72 | 3.79 | 1.28 |
| 25 | 3.95 | 3.96 | 3.95 | 3.96 | 3.96 | 0.13 |
| 30 | 3.98 | 4.02 | 4.03 | 4.00 | 4.01 | 0.45 |
| 35 | 4.01 | 4.03 | 4.03 | 4.02 | 4.02 | 0.37 |
| 40 | 3.93 | 3.90 | 3.96 | 3.88 | 3.91 | 0.77 |
| 45 | 3.87 | 3.85 | 3.90 | 3.86 | 3.87 | 0.48 |
| 50 | 3.64 | 3.64 | 3.66 | 3.62 | 3.64 | 0.41 |
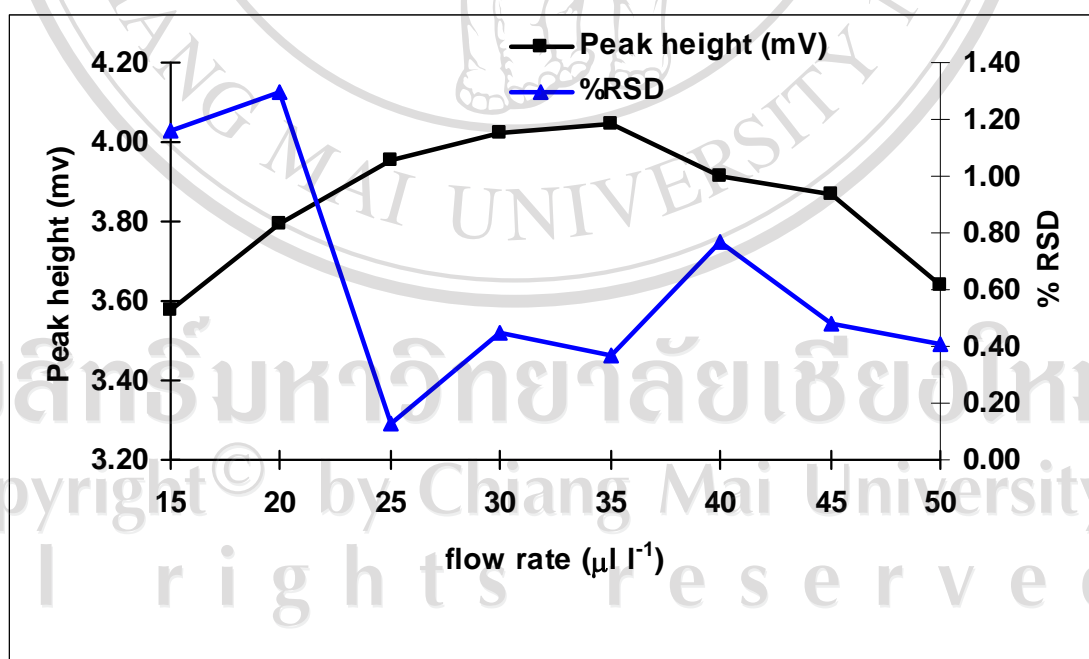


**Figure 3.18** Influence of flow rate of aspiration of sample on response and precision

**Table3.27** Influence of flow rate of aspiration of reagent on peak heights and precision

| Flow rate | Peak height (mV) | | | | | %RSD |
|:---:|:---:|:---:|:---:|:---:|:---:|:---:|
| ($\mu$l s$^{-1}$) | 1 | 2 | 3 | 4 | Mean | |
| 15 | 3.64 | 3.60 | 3.62 | 3.61 | 3.61 | 0.41 |
| 20 | 3.81 | 3.79 | 3.84 | 3.83 | 3.82 | 0.50 |
| 25 | 4.00 | 4.02 | 4.01 | 4.02 | 4.01 | 0.22 |
| 30 | 3.97 | 4.01 | 3.99 | 4.00 | 3.99 | 0.37 |
| 35 | 3.98 | 3.95 | 3.94 | 3.93 | 3.95 | 0.47 |
| 40 | 3.92 | 3.94 | 3.91 | 3.88 | 3.91 | 0.55 |
| 45 | 3.84 | 3.87 | 3.88 | 3.86 | 3.86 | 0.38 |
| 50 | 3.77 | 3.71 | 3.68 | 3.73 | 3.72 | 0.88 |
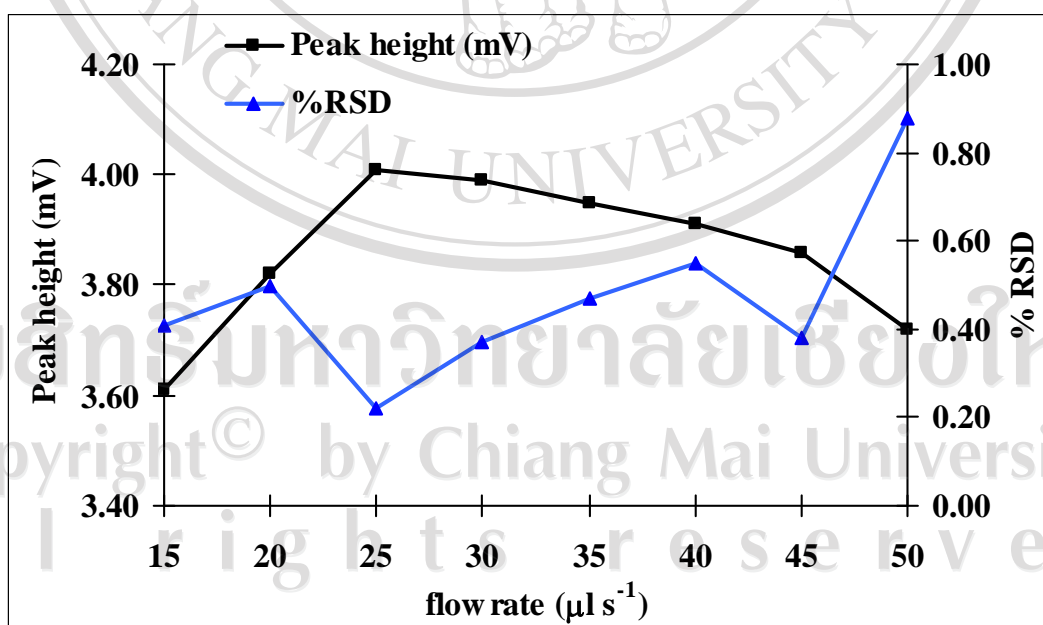


**Figure 3.19** Influence of flow rate of aspiration of reagent on peak heights and precision

### b) Flow Rate of Delivering Sample to Detector

The flow rates of sending the sample to detector were investigated from 15 – 50 µl s$^{-1}$ at every 5 µl s$^{-1}$ intervals the flow rate of aspiration of sample and reagent were kept constant at 25 µl s$^{-1}$. It was observed that the peak height increased with increasing in the flow rate up to 40 µl s$^{-1}$ and then it decreased with provision of the faster flow rates (Table 3.28 and Figure 3.20). Thus, a flow rate of 40 µl s$^{-1}$ was chosen and used for subsequent measurements due to its highest peak height and precision.

**Table 3.28** Influence of flow rate of delivering sample to detector

| Flow rate (µl s$^{-1}$) | Peak height (mV) | | | | | %RSD |
|---|---|---|---|---|---|---|
| | 1 | 2 | 3 | 4 | Mean | |
| 15 | 3.59 | 3.65 | 3.56 | 3.58 | 3.60 | 0.93 |
| 20 | 3.65 | 3.72 | 3.62 | 3.70 | 3.67 | 1.08 |
| 25 | 3.80 | 3.82 | 3.77 | 3.75 | 3.79 | 0.71 |
| 30 | 4.02 | 4.05 | 4.08 | 4.00 | 4.04 | 0.75 |
| 35 | 4.05 | 4.10 | 4.03 | 4.00 | 4.05 | 0.90 |
| 40 | 4.10 | 4.10 | 4.10 | 4.09 | 4.10 | 0.11 |
| 45 | 3.97 | 3.98 | 3.97 | 3.99 | 3.97 | 0.23 |
| 50 | 3.94 | 3.96 | 3.99 | 3.96 | 3.96 | 0.45 |
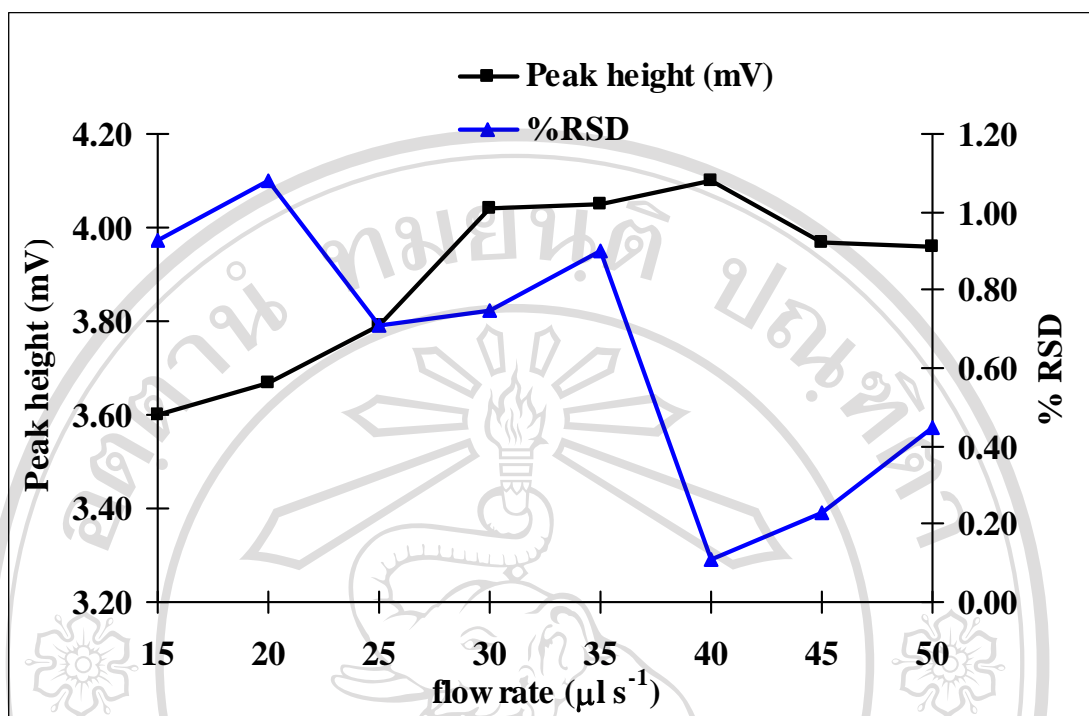
**Figure 3.20** Influence of flow rate of sending sample to detector

### 3.1.2.3.4 Sample and Reagents Aspiration Volumes Optimizations

To minimize the consumption of reagent volumes while maintaining the best results, both of sensitivity (slope) and precision, of the procedure, thus these parameters were optimized. The volumes of buffer solution, Triton X – 100, sample, PAN reagent and water were studied. When varying the volume of solution of interest whereas the others were kept constant at 50 $\mu l^{-1}$.

### a) Buffer Solution Aspiration Volume

The influence of the buffer volume was investigated in the range of 10 – 100 $\mu l$ at every 10 - $\mu l$ interval. There was no significant difference in the response when the volume increases. A buffer solution volume of 30 $\mu l$ was chosen as optimum due to

the precision and minimum volume of buffer solution consumed. The results are given in Table 3.29 and Figure 3.21.

### b) Triton X – 100 Volumes

The influence of the surfactant volume was studied in the range of $10 - 100$ µl at every 10 µl interval at the buffer solution aspiration volume of 30 µl. It was found that the peak height increased with increasing in surfactant volume up to 30 µl and at this volume, the high precision was obtained, thus the volume of surfactant (Triton X -100) was chosen at 30 µl. The results are given in Table 3.30 and Figure 3.22.

**Table 3.29** Influence of aspiration volume of buffer on peak heights and precision

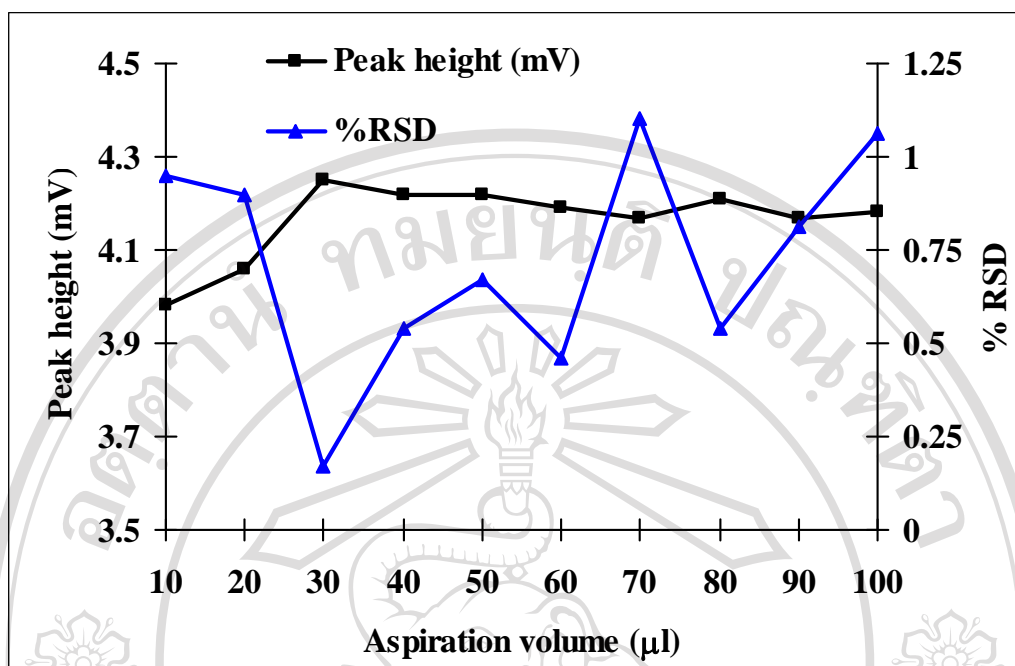| Aspiration volume (µl) | Peak height (mV) | | | | | %RSD |
|---|---|---|---|---|---|---|
| | 1 | 2 | 3 | 4 | Mean | |
| 10 | 3.97 | 3.92 | 4.02 | 4.02 | 3.98 | 0.95 |
| 20 | 4.05 | 4.01 | 4.10 | 4.07 | 4.06 | 0.90 |
| 30 | 4.24 | 4.25 | 4.26 | 4.25 | 4.25 | 0.19 |
| 40 | 4.22 | 4.20 | 4.19 | 4.25 | 4.22 | 0.54 |
| 50 | 4.19 | 4.25 | 4.19 | 4.24 | 4.21 | 0.65 |
| 60 | 4.18 | 4.16 | 4.20 | 4.21 | 4.19 | 0.46 |
| 70 | 4.20 | 4.15 | 4.23 | 4.11 | 4.17 | 1.10 |
| 80 | 4.19 | 4.21 | 4.25 | 4.21 | 4.21 | 0.54 |
| 90 | 4.18 | 4.15 | 4.12 | 4.21 | 4.17 | 0.81 |
| 100 | 4.13 | 4.24 | 4.21 | 4.15 | 4.18 | 1.06 |

**Figure 3.21** Influence of aspiration volume of buffer on peak heights and precision

**Table3.30** Influence of aspiration volume of Triton X-100 on peak heights and precision

| Aspiration volume (μl) | Peak height (mV) | | | | | %RSD |
|---|---|---|---|---|---|---|
| | **1** | **2** | **3** | **4** | **Mean** | |
| 10 | 4.01 | 4.03 | 4.07 | 4.09 | 4.05 | 0.86 |
| 20 | 4.05 | 4.13 | 4.03 | 4.10 | 4.08 | 0.97 |
| 30 | 4.07 | 4.08 | 4.06 | 4.08 | 4.08 | 0.20 |
| 40 | 4.07 | 4.10 | 4.09 | 4.12 | 4.10 | 0.44 |
| 50 | 4.05 | 4.12 | 4.14 | 4.04 | 4.09 | 1.06 |
| 60 | 4.06 | 4.05 | 4.05 | 4.09 | 4.06 | 0.40 |
| 70 | 4.09 | 4.02 | 4.06 | 4.12 | 4.07 | 0.91 |
| 80 | 4.08 | 4.02 | 4.00 | 4.13 | 4.06 | 1.27 |
| 90 | 4.02 | 4.07 | 4.11 | 4.14 | 4.09 | 1..10 |
| 100 | 4.13 | 4.07 | 4.01 | 4.09 | 4.08 | 1.07 |
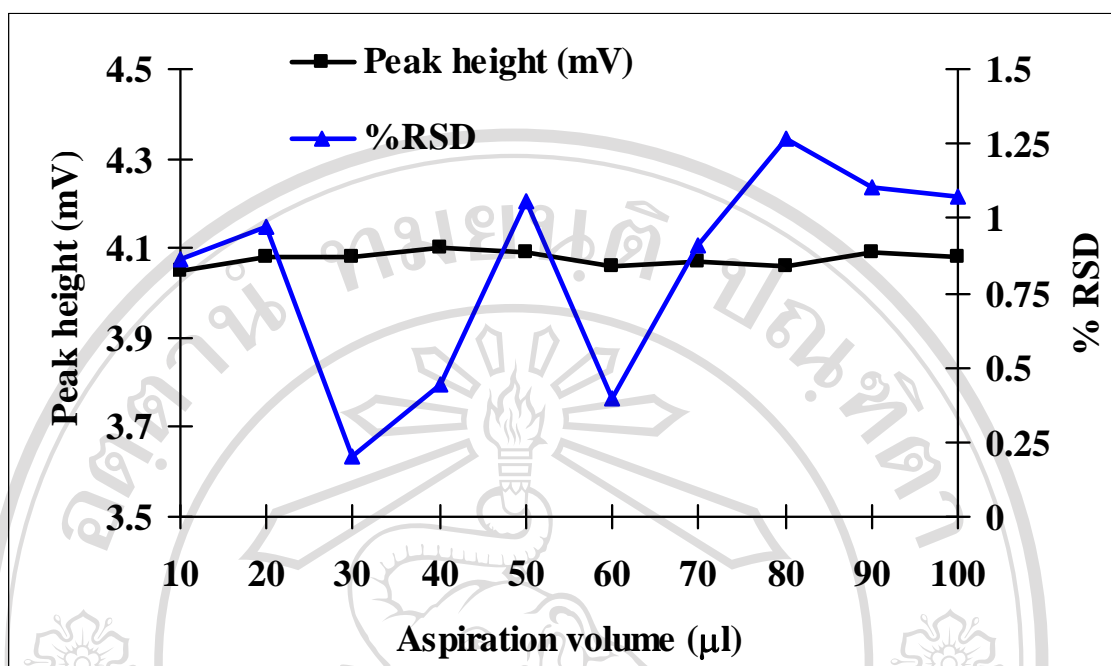
**Figure 3.22** Influence of aspiration volume of Triton – X 100r on peak heights and precision

#### c) Aspiration Volume of Sample Volumes

The influences of the sample and PAN reagent volumes were studied between 10 and 100 µl at every 10 µl interval. The volumes of buffer solution and surfactant were kept constant at 30 µl. It was found that the maximal response was obtained at a volume of 50 µl for sample volume and it gave the best precision (0.20% RSD). The results are given in Table 3.31 and Figure 3.23.

**Table3.31** Influence of aspiration volume of standard/sample on the peak heights and

precision

| Aspiration | Peak height (mV) | | | | | %RSD |
|:---:|:---:|:---:|:---:|:---:|:---:|:---:|
| volume (µl) | 1 | 2 | 3 | 4 | Mean | |
| 10 | 3.63 | 3.70 | 3.72 | 3.68 | 3.68 | 0.91 |
| 20 | 3.76 | 3.82 | 3.80 | 3.78 | 3.79 | 0.59 |
| 30 | 4.03 | 4.09 | 4.00 | 4.02 | 4.04 | 0.83 |
| 40 | 4.07 | 4.00 | 4.09 | 4.12 | 4.07 | 1.08 |
| 50 | 4.19 | 4.20 | 4.21 | 4.19 | 4.20 | 0.20 |
| 60 | 4.18 | 4.16 | 4.20 | 4.21 | 4.19 | 0.46 |
| 70 | 4.18 | 4.25 | 4.19 | 4.21 | 4.21 | 0.64 |
| 80 | 4.19 | 4.20 | 4.25 | 4.22 | 4.21 | 0.54 |
| 90 | 4.18 | 4.20 | 4.23 | 4.20 | 4.21 | 0.43 |
| 100 | 4.20 | 4.25 | 4.21 | 4.28 | 4.24 | 0.76 |
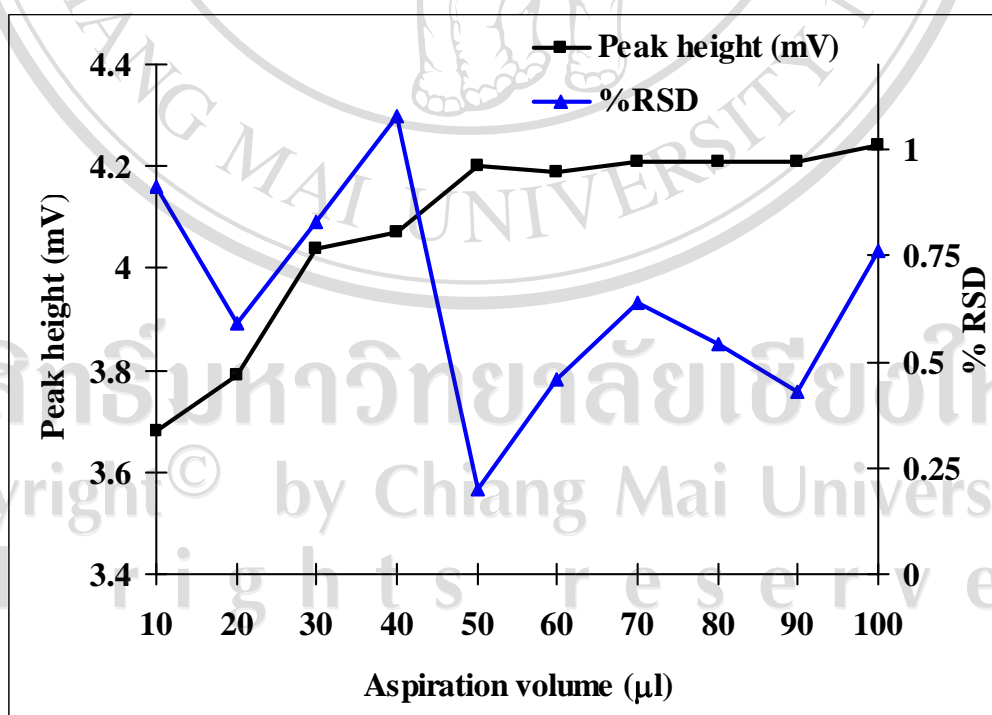


**Figure 3.23** Influence of aspiration volume of standard/sample on the peak heights

and precision

**d) Aspiration Volume of PAN**

The influence of the sample and PAN reagent volumes were studied between 10 and 100 µl at every 10µl interval. The volumes of buffer solution, surfactant and standard/sample were kept constant at 30, 30 and 50 µl respectively. For PAN reagent volume, it was found that as the aspiration volume increased the peak height increased up to 30 µl and remained almost constant afterwards. A volume of 30 µl was chosen as an optimum reagent volume for subsequent measurements. In addition, this volume gave a fine base line in SIA grams. The results are given in Table 3.32 and Figure 3.24.

**Table 3.32** Influence of aspiration volume of PAN on the peak heights and precision

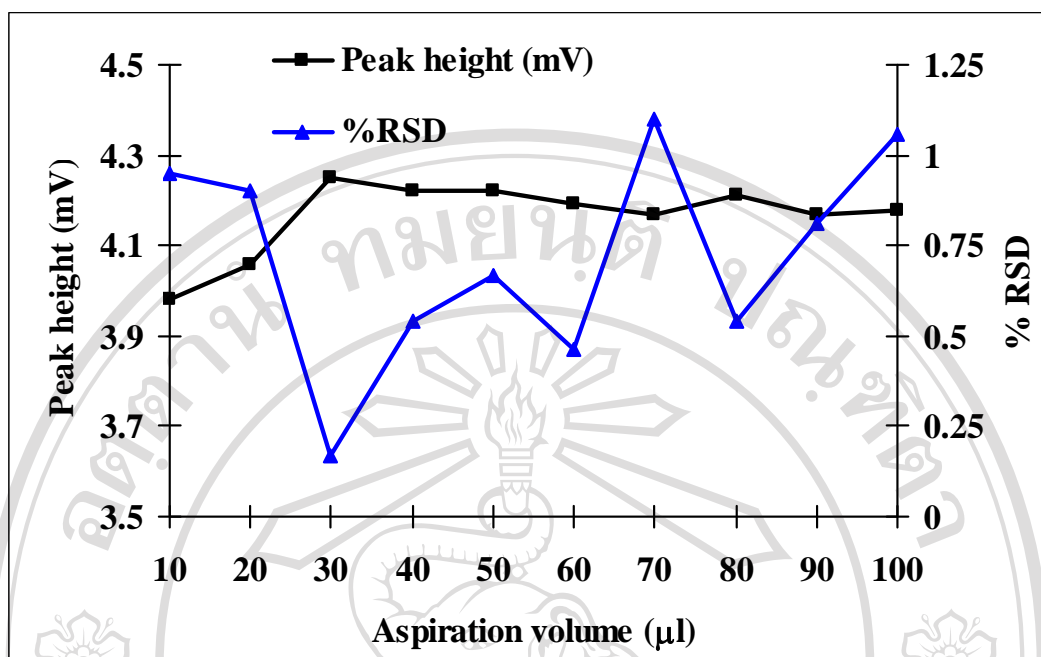| Aspiration volume (µl) | Peak height (mV) | | | | | %RSD |
|---|---|---|---|---|---|---|
| | 1 | 2 | 3 | 4 | Mean | |
| 10 | 3.97 | 3.92 | 4.00 | 4.02 | 3.98 | 0.95 |
| 20 | 4.05 | 4.00 | 4.10 | 4.07 | 4.06 | 0.90 |
| 30 | 4.24 | 4.25 | 4.26 | 4.25 | 4.25 | 0.17 |
| 40 | 4.22 | 4.20 | 4.19 | 4.25 | 4.22 | 0.54 |
| 50 | 4.19 | 4.25 | 4.19 | 4.24 | 4.22 | 0.67 |
| 60 | 4.18 | 4.16 | 4.20 | 4.21 | 4.19 | 0.46 |
| 70 | 4.20 | 4.15 | 4.23 | 4.11 | 4.17 | 1.10 |
| 80 | 4.19 | 4.20 | 4.25 | 4.21 | 4.21 | 0.54 |
| 90 | 4.18 | 4.15 | 4.12 | 4.21 | 4.17 | 0.81 |
| 100 | 4.13 | 4.24 | 4.21 | 4.15 | 4.18 | 1.06 |

**Figure 3.24** Influence of aspiration volume of PAN on the peak heights and precision

### 3.2.1.3.5 The Effect of PAN Concentrations

The effect of PAN concentration was studied in the range $1.0 \times 10^{-5}$ to $2.0 \times 10^{-6}$ mol l$^{-1}$. The peak height increases with increasing concentration up till $5 \times 10^{-5}$ mol l$^{-1}$ and started leveling off [Figure 3.25 and Table 3.33]. The concentration of PAN at 5.0 $\times 10^{-5}$ mol l$^{-1}$ and $10 \times 10^{-5}$ mol l$^{-1}$ have the best peak heights but the % RSD at 5.0 $\times 10^{-5}$ mol l$^{-1}$ is lower than that obtained at $10 \times 10^{-5}$ hence the $5 \times 10^{-5}$ mol l$^{-1}$ PAN was chosen for further works.

**Table 3.33** Influence of PAN concentration on peak heights and precision

| [PAN] x 10$^{-5}$ mol l$^{-1}$ | Peak height (mV) | | | | | %RSD |
|---|---|---|---|---|---|---|
| | 1 | 2 | 3 | 4 | Mean | |
| 1.0 | 4.75 | 4.80 | 4.73 | 4.71 | 4.74 | 0.70 |
| 2.5 | 4.90 | 4.82 | 4.95 | 4.85 | 4.88 | 1.01 |
| 5.0 | 5.30 | 5.32 | 5.29 | 5.34 | 5.31 | 0.36 |
| 7.5 | 5.10 | 5.06 | 5.19 | 5.12 | 5.12 | 0.92 |
| 10.0 | 5.20 | 5.23 | 5.20 | 5.29 | 5.23 | 0.70 |
| 12.5 | 5.19 | 5.30 | 5.22 | 5.17 | 5.22 | 0.95 |
| 15.0 | 5.30 | 5.13 | 5.19 | 5.27 | 5.22 | 1.28 |
| 17.5 | 5.20 | 5.11 | 5.27 | 5.09 | 5.17 | 1.40 |
| 20.0 | 5.10 | 5.18 | 5.29 | 5.27 | 5.21 | 1.46 |
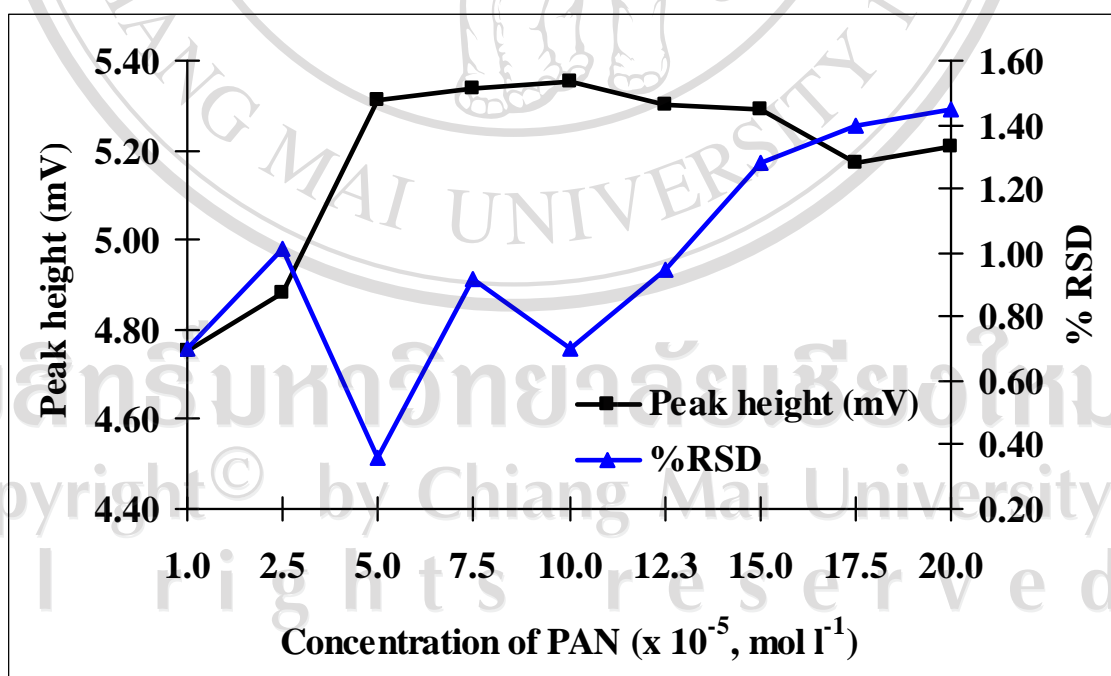


**Figure 3.25** Influence of PAN concentration on peak heights and precision

### 3.2.1.3.6 The Effect of Concentration of Triton X – 100

Preliminary experiments revealed that suitable conditions for dissolving Zn(II) – PAN complex in aqueous solution by adding some non – ionic surfactants such as Tween – 80, Triton X – 100, poly(vinylalcohol) were successively added at different concentrations ( 0.1 – 1.0 % v/v). Preliminary experiments pointed out that cationic surfactants could not be added. In fact, the analytical signal was not observed in the presence of cetyltrimethylammonium or cetrypriridinium chloride, in view of the hydration caused by the ionic group [31]. That reduced the molecular forces impairing the dissolution, thus the establishment of the organized medium. Cationic surfactants were then not investigated further. Among the different non – ionic surfactant tested, Triton X – 100 was selected because the attainable sensitivity was higher.

Without addition of surfactant, Zn (II) – PAN complex cannot be dissolved in aqueous phase thus in the system the precipitate can accumulate on the tubing inner wall and flow cell, impairing the instrumentation of the method. Concentration of this surfactant plays an important role in the system designed. For concentration higher than 0.0130 % v/v (critical micelle concentration), the products formed aggregated themselves. The influence concentration of Triton X – 100 was studied over the range 0.1 – 1.0 % v/v. The response increased with an increase in concentration, the 1.0 % v/v concentration was chosen for the best peak height and good precision of the method [Table 3.34 and Figure 3.26]. The higher concentration than 1.0 %v/v did not recommend because it caused high viscosity and the peak height did not relate with sample concentration**.**

**Table 3.34** Influence of Triton X-100 concentration on peak heights and precision

| Triton X-100 % v/v | Peak height (mV) | | | | | %RSD |
| --- | --- | --- | --- | --- | --- | --- |
| | 1 | 2 | 3 | 4 | Mean | |
| 0.1 | 4.75 | 4.80 | 4.73 | 4.71 | 4.75 | 0.70 |
| 0.2 | 4.90 | 4.82 | 4.95 | 4.85 | 4.88 | 1.01 |
| 0.3 | 5.30 | 5.32 | 5.29 | 5.34 | 5.31 | 0.36 |
| 0.4 | 5.43 | 5.48 | 5.49 | 5.42 | 5.46 | 0.47 |
| 0.5 | 5.51 | 5.49 | 5.54 | 5.57 | 5.53 | 0.55 |
| 0.6 | 5.59 | 5.52 | 5.58 | 5.55 | 5.56 | 0.49 |
| 0.7 | 5.64 | 5.62 | 5.69 | 5.60 | 5.64 | 0.59 |
| 0.8 | 5.69 | 5.71 | 5.68 | 5.73 | 5.70 | 0.34 |
| 0.9 | 5.77 | 5.74 | 5.79 | 5.73 | 5.76 | 0.41 |
| 1.0 | 5.86 | 5.87 | 5.84 | 5.83 | 5.85 | 0.66 |
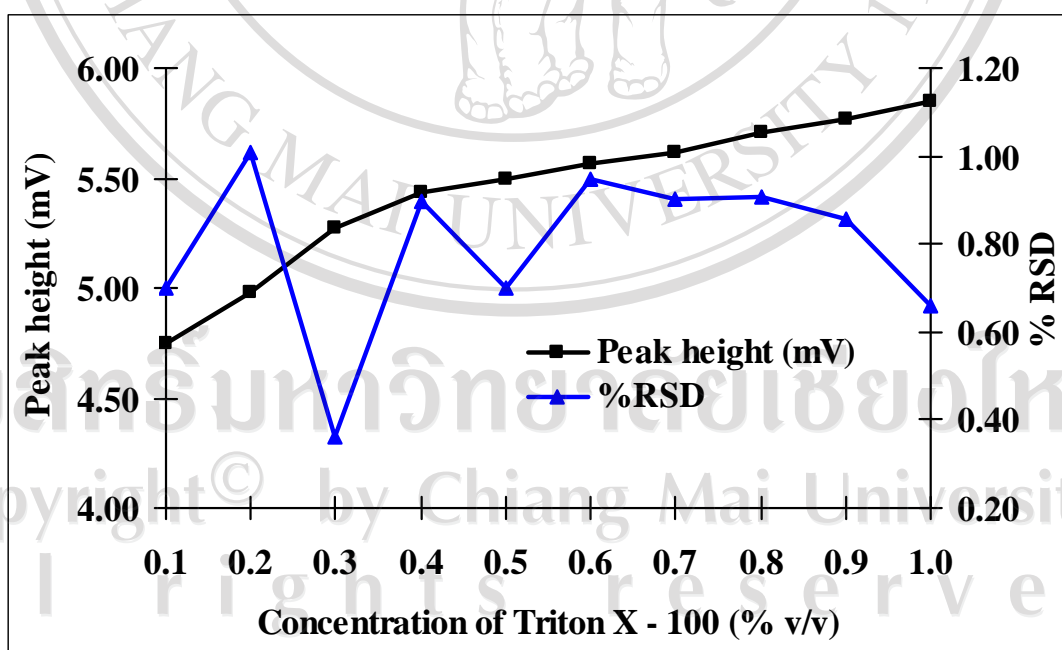


**Figure 3.26** Influence of Triton X – 100 concentrations of peak heights and precision

### 3.2.2 Analytical Characteristics

#### 3.2.2.1 Linear Range

Using the optimized parameters listed in Table 3.35, the SIA system was evaluated for its response for different concentrations of standard zinc solutions. The linear range was studied by measurement of various concentrations of zinc standard condition; $0.1 - 5.0$ µg ml$^{-1}$. The results obtained are shown in Table 3.36 and Figure3.27. It was found that a linear working calibration curve ranging from $0.1 - 1.0$ µg ml$^{-1}$ of zinc (II) solution was obtained.

**Table 3.35** Optimization parameters

| parameters | Optimized value |
|---|---|
| pH of carbonate buffer solution | 9.5 |
| Flow rate | |
|    - Flow rate of aspiration of sample and reagents | 25 µl s$^{-1}$ |
|    - Flow rate of sending sample to detector | 40 µl s$^{-1}$ |
| Buffer aspiration volumes | 30 µl |
| Triton X - 100 aspiration volumes | 30 µl |
| Sample aspiration volumes | 50 µl |
| PAN reagent aspiration volumes | 30 µl |
| PAN concentration | 5 X 10$^{-5}$ mol l$^{-1}$ |
| Triton X – 100 concentration | 1 % v/v |
| Reaction coil diameter | 0.7 mm |
| Wavelength | 553 nm |
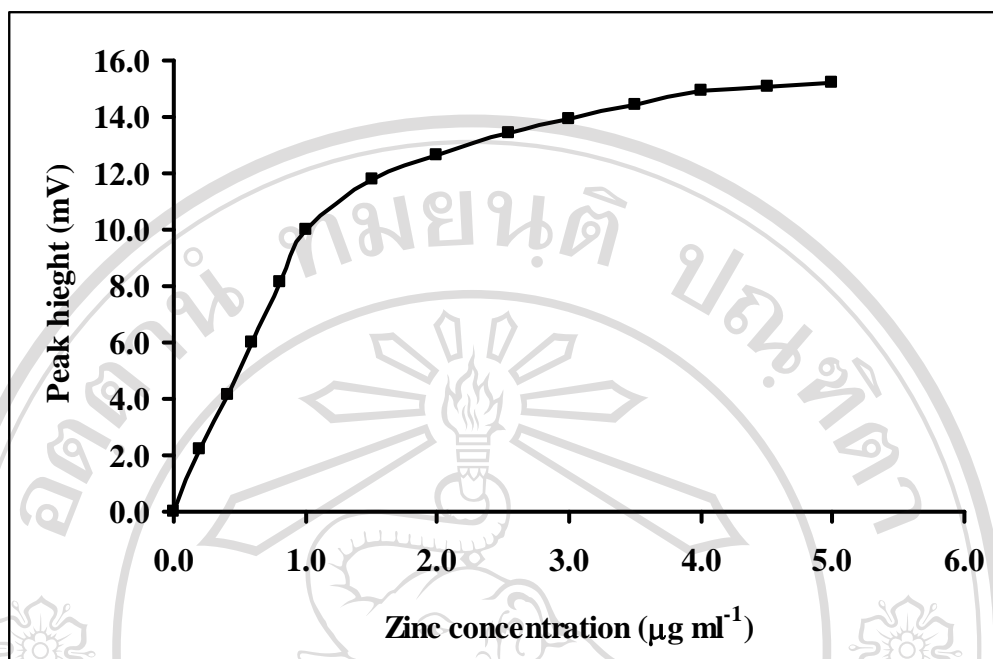
**Figure 3.27** The curve showing the linear range for zinc (II) determination

**Table3.36** Peak height at various zinc (II) concentrations for linearity checking of the calibration curve

| Zinc(II) concentration ($\mu$g ml$^{-1}$) | Peak height[*] (mV) |
|---|---|
| 0.0 | 0.02 |
| 0.2 | 2.46 |
| 0.4 | 4.41 |
| 0.6 | 6.58 |
| 0.8 | 8.67 |
| 1.0 | 10.64 |
| 1.5 | 11.82 |
| 2.0 | 12.67 |
| 2.5 | 13.45 |
| 3.0 | 14.04 |
| 3.5 | 14.57 |
| 4.0 | 15.04 |
| 4.5 | 15.13 |
| 5.0 | 15.27 |

[*] Average from four determinations

### 3.2.2.2 Calibration Curve and Detection Limit

Under the optimum conditions, the calibration curve was linear between 0.1 – 1.0 µg ml$^{-1}$ with the following calibration equation: *Y = 10.714X +0.0837*, with a correlation coefficient ($R^2$) of 0.9993, where *Y* and *X* represented SIA signal as peak height in mV, and zinc (II) concentrations in µg ml$^{-1}$ respectively. The limit of detection was calculated ($3\sigma$, $\sigma$ is the standard deviation of the blank (n = 10)) is 0.02 µg ml$^{-1}$. The limit of quantification was calculated ($10\sigma$) is 0.06 µg ml$^{-1}$. The Figures 3.28 - 3.29 show the SIA gram and calibration curve for zinc determination.
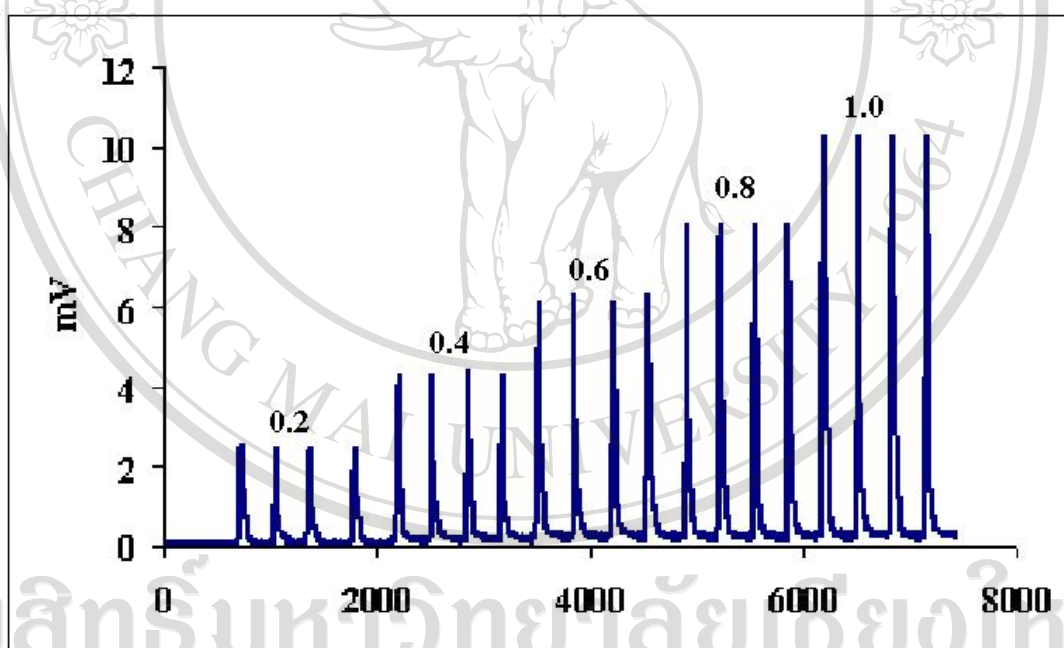


**Figure 3.28** SIA gram for zinc (II) determination
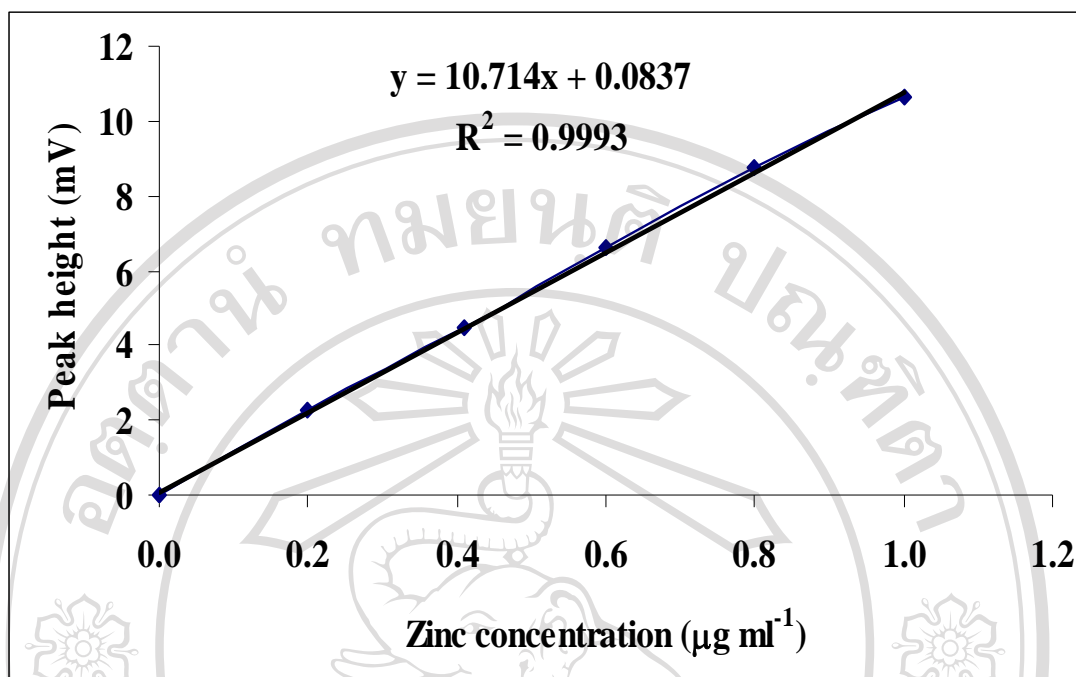
**Fig 3.29** Calibration curve for zinc (II) determination

### 3.2.2.3 Repeatability and Reproducibility

The repeatability of the method was checked for 0.1and 0.5 µg ml$^{-1}$ (Fig 3.29) standard solution, the R.S.D. values of 2.27 and 1.25, respectively, were registered ($n$ = 10 measurements in each case). The reproducibility of the method was pursed by determining 10 standard solutions of 0.1 and 0.5µg ml$^{-1}$. The results obtained are summarized in Tables 3.37- 3.38, the R.S.D. values of 2.39 and 1.29, respectively. The sample throughput was 40 h$^{-1}$.
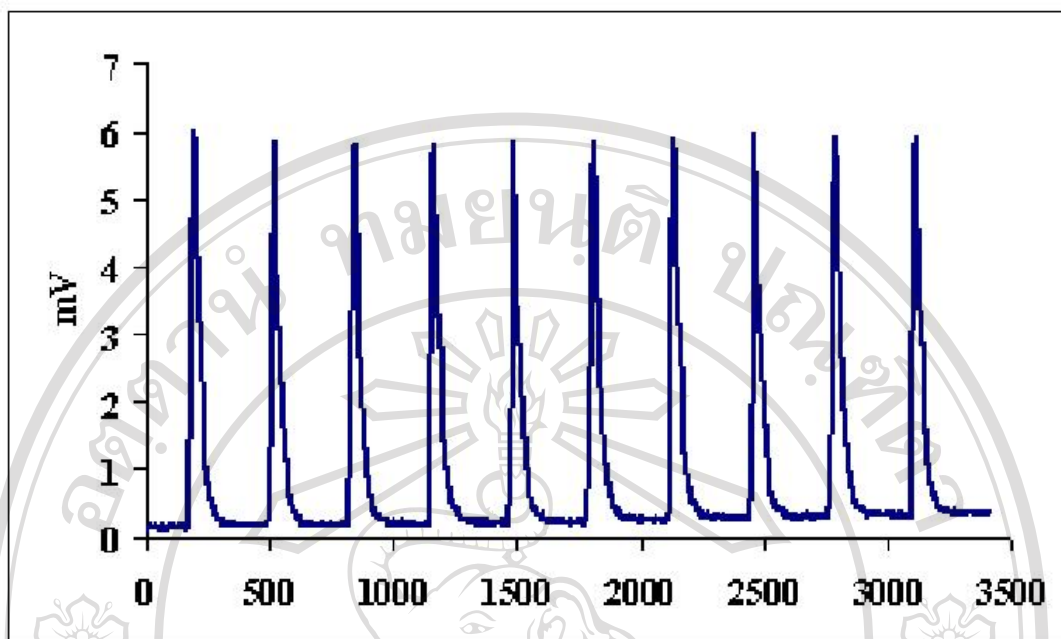
**Figure 3.30** SIA gram for 0.5 µg ml$^{-1}$

### 3.2.3 Interference Study

The effects of metallic ion interferences on the determination of 1 µg ml$^{-1}$ zinc (II) using the proposed method were tested. Results are summarized in Table 3.39. The tolerance limit was taken as the concentration of the added ion causing less than 3 % relative error.

Fe(III), Mn(II) and Ca(II) are possible interfering species in this method. The interfering species were eliminated by using appropriate masking agent and pH values Fe(III) by the addition of sodium fluoride, Mn(II) and Ca(II) by addition of potassium cyanide as masking agent, and the careful control of the pH of the buffer solution.

**Table 3.37** Repeatability and reproducibility of replicate determination of 0.1 µg ml$^{-1}$

zinc (II)

| Experiment | Peak height* (mV) | |
| :---: | :---: | :---: |
| number | **Repeatability** | **Reproducibility** |
| 1 | 1.68 | 1.65 |
| 2 | 1.62 | 1.67 |
| 3 | 1.59 | 1.58 |
| 4 | 1.65 | 1.64 |
| 5 | 1.69 | 1.62 |
| 6 | 1.63 | 1.59 |
| 7 | 1.67 | 1.54 |
| 8 | 1.63 | 1.63 |
| 9 | 1.61 | 1.59 |
| 10 | 1.58 | 1.63 |
| **Average** | **1.64** | **1.61** |
| **Standard deviation** | **0.037** | **0.039** |
| **% RSD** | **2.27** | **2.39** |

*Average of 4 repetitive determinations

**Table 3.38** Repeatability and reproducibility of replicate determination of 0.5 µg ml$^{-1}$ zinc (II)

| Experiment number | Peak height* (mV) | |
|---|---|---|
| | Repeatability | Reproducibility |
| 1 | 6.15 | 6.11 |
| 2 | 5.97 | 6.04 |
| 3 | 5.94 | 5.98 |
| 4 | 6.07 | 6.14 |
| 5 | 5.98 | 6.07 |
| 6 | 6.12 | 5.97 |
| 7 | 5.97 | 6.03 |
| 8 | 6.07 | 6.12 |
| 9 | 6.13 | 5.94 |
| 10 | 6.05 | 6.17 |
| **Average** | **6.05** | **6.06** |
| **Standard deviation** | **0.076** | **0.078** |
| **% RSD** | **1.25** | **1.29** |

* Average of 4 repetitive determinations

**Table 3.39** Tolerance limits of interferences ions on the determination of 1 $\mu g\ ml^{-1}$

zinc at optimum conditions

| Ion | Tolerated ratio of interferences ions to zinc(II) |
|---|---|
| $Ca^{2+}$, $Mg^{2+}$, $Al^{3+}$ | 500* |
| $Cu^{2+}$, $Co^{2+}$, $Ni^{2+}$ | 750* |
| $Fe^{3+}$, $Mn^{2+}$ | 50 |
| $Cd^{2+}$ | 75 |
| $Pb^{2+}$ | 250* |
| $Cr^{2+}$, $Ag^+$, $Hg^{2+}$ | 550 |
| $I^-$, $Cl^-$ | 1000 |

* More than these amounts of ions cause precipitation

### 3.2.4 Determination of Zinc (II) in Pharmaceutical Preparations

The developed SIA method has been satisfactorily applied to the determination of zinc (II) in commercial pharmaceutical preparations. Centrum tablets were analyzed (Table 3.40). Comparative determination of zinc (II) in the sample solutions by atomic absorption spectrophotometry (AAS) was also carried out. Results obtained by the proposed SIA and AAS methods were compared favorably verified by the Student *t*- test.

**Table3.40** Determination of zinc (II) in pharmaceutical preparations sample with the

propose SIA method and flame atomic absorption spectrophotometric method

| *Sample | SIA (mg /tablet) (n=5) | FAAS (mg/tablet) (n=5) | Calculated $t$- test value | % labeled amount |
|---------|------------------------|------------------------|----------------------------|------------------|
| S 1 | $15.06 \pm 0.21$ | $14.89 \pm 1.25$ | 0.60 | 100.40 |
| S 2 | $14.90 \pm 0.95$ | $15.01 \pm 0.60$ | 0.27 | 99.33 |
| S 3 | $15.08 \pm 0.60$ | $15.11 \pm 1.18$ | 0.13 | 100.53 |
| S 4 | $15.11 \pm 1.03$ | $15.09 \pm 1.09$ | 0.46 | 100.73 |
| S 5 | $15.13 \pm 0.96$ | $15.16 \pm 0.97$ | 0.38 | 100.87 |
| S 6 | $15.07 \pm 1.12$ | $14.89 \pm 0.85$ | 0.58 | 100.47 |
| S 7 | $14.91 \pm 1.03$ | $15.07 \pm 1.04$ | 0.29 | 99.04 |

*The claimed value for all samples was 15 mg per tablet.

## 3.3 Determination of Active Ingredients in Cough – Cold Pharmaceutical Preparations by Micellar Liquid Chromatography
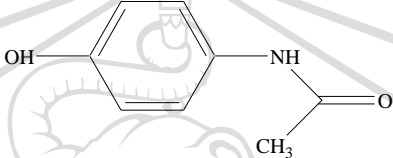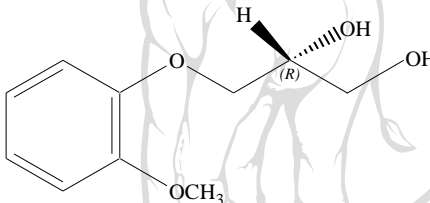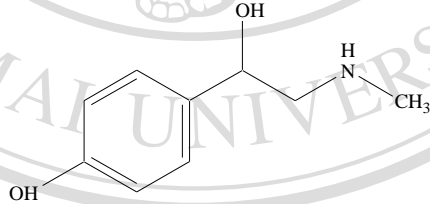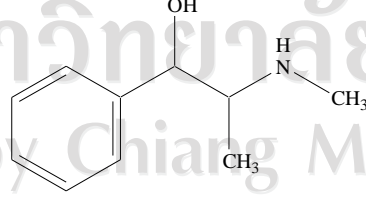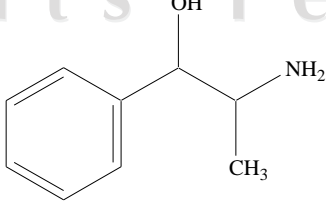
Micellar liquid chromatography (MLC) is a useful technique to perform some separations involving mixtures of compounds with different hydrophobicities without the need of using a gradient. The retention of analytes in the column with pure micelle eluents (without modifier) was high. Thus, the addition of a small amount of organic solvent was convenient to decrease the retention time. The presence of small amounts of organic additive in the micellar mobile phase can have an important impact on the

association of micells and can be useful in the elution of retained compounds. An adequate control of surfactant and modifier concentrations can lead to chromatograms showing a good resolution in the analysis of compounds with different hydrophobicities.

For more hydrophobic drugs studied, the retention changes largely with increasing the surfactant concentration. But if the surfactant concentration is sufficiently high, the layer produced on the stationary phase is so dense that it reduces efficiency due to the decrease in the mass transfer rate from the stationary phase. On the other hand, an increase in the organic solvent concentration always improves efficiency because it reduces the capacity factor of the analytes due to the elimination of the monomers in the stationary phase. In order to reach a compromise between these two interactive factors, a simultaneous optimization strategy based on an iterative regression process was performed. Optimization of these parameters was based on the criteria of greater separation efficiency, peak area and shorter analysis time.

The aim of this work was to develop a rapid and simple procedure for the determination of the combinations cough – cold drugs that are administered in USA, using a limited number of mobile phases. For this purpose, the chromatographic behavior of the drugs was examined on the $C_8$ column. Mixtures of the acetaminophen, guaifenesin, phenylephrine, pseudoephedrine and phenylpropanolamine, (Table 3.41) were considered. Mobile phase selection was made with the aid of an optimization strategy based on the modeling of the retention and peak shape. The results are compared with those obtained by using an optimized mobile phase of methanol–water.

**Table 3.41** Structures, dissociation constants and octanol-water partition constants of acetaminophen, guaifenesin, phenylephrine, pseudoephedrine and phenylpropanolamine

| compound | structure | logP o/w | pKa |
|---|---|---|---|
| Acetaminophen |  | 0.28 | 15.32(NH) 10.82(OH) |
| Guaifenesin |  | 0.73 | 14.99 13.45 |
| Phenylephrine |  | -0.09 | 8.9 |
| Pseudoephedrine |  | 0.89 | 9.5 |
| Phenylpropanolamine |  | 0.58 | 9.4 |

### 3.3.1 Development and Optimization of the Micellar Liquid Chromatographic

Preliminary experiments were carried out to optimize the main parameters affecting the MLC. Optimization was necessary to achieve complete separation of the compounds in the short time and to eliminate possible matrix interferences. In this work the wavelength selection, effect of concentration of SDS, effect of concentration of organic modifier, pH and flow rate were investigated.

#### 3.3.1.1 Wavelength Selection

The aim of this work was to develop a micellar HPLC procedure for the determination of five drugs simultaneously using UV detector. Therefore, a suitable wavelength for detection of these drugs was investigated in order to achieve high sensitivity. A standard mixture containing acetaminophen (20 μg ml$^{-1}$) guaifenesin (20 μg ml$^{-1}$) phenylephrine (50 μg ml$^{-1}$), pseudoephedrine (50 μg ml$^{-1}$) and phenylpropanolamine (50 μg ml$^{-1}$) was injected and separated on the column (150 x 4.6 mm i.d) packed with C8 (5 μm) using 0.150 mol ml$^{-1}$ SDS- 2.0 % v/v pentanol as mobile phase with a flow rate of 1.0 ml min$^{-1}$. The UV spectrum of each standard drug showed the absorption maxima about 254 nm and at approximately 200-210 nm with the greater absorbance. Therefore, wavelength of 210 nm and 254 nm were taken into consideration. After investigation by MLC, the peak areas from 210 and 254 nm were listed in Table 3.42. It was found that the peak areas of these drugs at 210 nm were greater than peak area at 254 nm. So, the wavelength of 210 nm was selected as optimal wavelength to monitor these drugs.

Table3.42 Comparison of peak area between the wavelength of 210 nm and 254 nm

| Compounds | Peak area (mAU * s) | |
|---|---|---|
| | 210 nm | 254 nm |
| Acetaminophen | 1754 | 945 |
| Guaifenesin | 2621 | 452 |
| Phenylephrine | 2774 | 357 |
| pseudoephedrine | 1529 | 2201 |
| phenylpropanolamine | 1875 | 1579 |

### 3.3.1.2 Effect of SDS Concentration

The surfactant concentration affects the elution strength in the mobile phase using MLC. In this case, the optimization was developed using a standard solutions containing acetaminophen (20 µg ml$^{-1}$) guaifenesin (20 µg ml$^{-1}$) phenylephrine (50 µg ml$^{-1}$), pseudoephedrine (50 µg ml$^{-1}$) and phenylpropanolamine (50 µg ml$^{-1}$). The SDS concentration range of 0.025 – 0.150 mol 1$^{-1}$ was varied while an initial pH 3, a flow rate of 1 ml min$^{-1}$ and 2.0 % concentration of pentanol were kept constant. From the peaks that were obtained in these concentrations, measurements of different parameters for each of the standards were determined. These data are shown in Table 3.43. It was found that the elution order of the assayed drugs was acetaminophen, guaifenesin, phenylephrine, pseudoephedrine and phenylpropanolamine for all the mobile phases inside the experimental domain. When the SDS concentration was increased the retention times decreased owing to a larger

number of micelles in the mobile phase. Finally, the analysis time taken as the time needed to elute completely the most retained compound on the stationary phase was 38 min for the weakest mobile phase (0.025 mol $l^{-1}$), and 14 min for the strongest one (0.150 mol $l^{-1}$). A mobile phase containing 0.15 mol $l^{-1}$ SDS was selected to analyse the pharmaceuticals, which correspond to the highest concentrations assayed. It should be noted that the upper surfactant concentration is determined by its solubility and the viscosity of the resulting mobile phase. The retention times for the drugs eluted with 0.15 mol $l^{-1}$ - SDS–2% pentanol were:  acetaminophen (1.833 min), guaifenesin (3.348 min), phenylephrine (5.859 min), pseudoephedrine (9.184 min) and phenylpropanolamine (10.517 min), respectively.

### 3.3.1.3 Effect of Pentanol Concentration

The retention of analysis compounds was high in a pure micellar chromatographic system (without modifier).  A strong organic modifier added to the SDS mobile phase was therefore needed to elute the drugs from the columns. In this work, using a small amount of pentanol was shown to decrease the retention times of strongly retained solute in $C_8$ columns to adequate values. In this work, it is about green analytical chemistry, which is using organic solvent as less as possible thus, pentanol was used in small amount as modifier organic solvent compared with others alcohols. Finally pentanol was used as modifier for this MLC system.

The suitable concentration of pentanol was studied when the mobile phases contained 0.150 mol $l^{-1}$ SDS with the flow rate 1.0 ml $min^{-1}$. The results were demonstrated in Table 3.44 and it was found that if the concentration of pentanol was higher than 2.5 %v/v, the separation efficiency was poor in the resolution of the

pseudoephedrine and phenylpropanolamine peaks. Comparing the results obtained from the presence of 1.5 % v/v and 2.0 %v/v pentanol in the mobile phases, the analysis time of the system at 2.0 %v/v was shorter than that obtained at 1.5 % v/v, they were 13 and 17 min, respectively. Thus, 2.0 %v/v of pentanol was selected as optimum mobile phase for the simultaneous separation and determination these drugs.

**Table3.43** Effect of concentration of SDS

| [SDS] , mol l$^{-1}$ | Drugs | Chromatographic behaviors | | | | |
|---|---|---|---|---|---|---|
| | | $t_R$ (mins) | Area (mAU *s) | $W_{1/2}$ (min) | k' | Rs |
| 0.025 | Acetaminophen | 2.114 | 1750 | 0.045 | 2.989 | - |
| | Guaifenisin | 4.699 | 2782 | 0.081 | 7.866 | 20.5 |
| | Phenylephrine | 17.810 | 3374 | 0.267 | 32.604 | 37.7 |
| | Pseudoephedrin | 31.203 | 1534 | 0.469 | 57.874 | 19.0 |
| | Phenylpropanolamine | 33.465 | 2007 | 0.487 | 62.142 | 2.36 |
| 0.050 | Acetaminophen | 2.044 | 1769 | 0.039 | 2.813 | - |
| | Guaifenisin | 4.470 | 2941 | 0.081 | 7.215 | 20.2 |
| | Phenylephrine | 13.180 | 3667 | 0.216 | 25.321 | 29.3 |
| | Pseudoephedrin | 21.665 | 1631 | 0.368 | 36.311 | 14.5 |
| | Phenylpropanolamine | 24.290 | 2070 | 0.395 | 48.210 | 3.4 |
| 0.075 | Acetaminophen | 1.995 | 1658 | 0.057 | 2.764 | - |
| | Guaifenisin | 4.174 | 2790 | 0.081 | 6.875 | 15.8 |
| | Phenylephrine | 9.670 | 3107 | 0.164 | 17.245 | 22.4 |
| | Pseudoephedrin | 15.951 | 1566 | 0.281 | 29.096 | 14.1 |
| | Phenylpropanolamine | 18.175 | 1986 | 0.301 | 33.292 | 3.8 |
| 0.100 | Acetaminophen | 1.893 | 1802 | 0.064 | 2.572 | - |
| | Guaifenisin | 3.697 | 2810 | 0.077 | 5.975 | 12.8 |
| | Phenylephrine | 7.671 | 3003 | 0.140 | 13.473 | 18.3 |
| | Pseudoephedrin | 12.195 | 1602 | 0.227 | 22.009 | 12.3 |
| | Phenylpropanolamine | 13.683 | 2061 | 0.248 | 24.817 | 3.13 |
| 0.125 | Acetaminophen | 1.874 | 1780 | 0.062 | 2.536 | - |
| | Guaifenisin | 3.581 | 2740 | 0.080 | 5.757 | 12.0 |
| | Phenylephrine | 7.172 | 2977 | 0.140 | 12.532 | 16.3 |
| | Pseudoephedrin | 11.694 | 1570 | 0.231 | 21.064 | 12.2 |
| | Phenylpropanolamine | 13.624 | 1987 | 0.254 | 24.706 | 4.0 |
| **0.150** | **Acetaminophen** | **1.833** | **1771** | **0.089** | **2.458** | **-** |
| | **Guaifenisin** | **3.348** | **2695** | **0.077** | **5.317** | **9.1** |
| | **Phenylephrine** | **5.859** | **2853** | **0.118** | **10.055** | **12.9** |
| | **Pseudoephedrin** | **9.184** | **1550** | **0.186** | **16.328** | **10.9** |
| | **Phenylpropanolamine** | **10.517** | **1967** | **0.198** | **18.840** | **3.5** |

### 3.3.1.4 Effect of Flow Rate

The mobile phase flow rate for cough-cold drugs determination was optimized by using 0.150 mol $l^{-1}$ SDS with 2.0 %v/v pentanol at various flow rates; 0.8, 0.9, 1.0, 1.1, 1.2, 1.3, 1.4 and 1.5 ml $min^{-1}$ (Table 3.45). It was clear that the higher mobile phase flow rate, the shorter retention time and the worse resolution factor were obtained. Consider the highest flow rate, 1.5 ml $min^{-1}$, the retention times of these drugs were: acetaminophen (1.296 min), guaifenesin (2.471 min), phenylephrine (4.370 min), pseudoephedrine (7.081 min) and phenylpropanolamine (8.280 min) respectively. At this flow rate, the resolution of the pseudoephedrine and phenylpropanolamine was separated completely. Thus, the optimized flow rate for determination of these drugs is 1.5 ml $min^{-1}$.

### 3.3.1.5 Effect of pH

The mixture of investigated compounds consisted of five compounds (acetaminophen, guaifenesin, phenylephrine, pseudoephedrine and phenylpropanolamine), is weakly acidic with pK = 8.9 – 13.45 (Table 3.41). They do not show any acid–base behavior in the working pH range of the C8 column. The change in retention factors of the investigated compounds with pH in a micellar mobile phase of 0.150 M SDS–2.0% (v/v) pentanol is shown in Figure 3.31. The retention of acetaminophen, guaifenesin, phenylephrine, pseudoephedrine and phenylpropanolamine practically did not change over the pH range 2–7. In a micellar chromatographic system with the anionic SDS, the stronger attraction of the doubly charged cationic drugs to the surfactant adsorbed on the stationary phase, with respect to the micelles in the mobile phase, increases their retention at decreasing pH. The

following series and the determination of the drugs in the pharmaceuticals were performed at pH 7, because of the shorter retention time.

**Table 3.44** Effect of concentration pentanol

| Pentanol Conc. (%v/v) | Drugs | Chromatographic behaviors | | | | |
|---|---|---|---|---|---|---|
| | | $t_R$ (mins) | Area (mAU *s) | $W_{1/2}$ (min) | $k'$ | Rs |
| 1.5 | Acetaminophen | 1.969 | 1765 | 0.068 | 2.750 | - |
| | Guaifenisin | 4.122 | 2547 | 0.069 | 6.851 | 15.7 |
| | Phenylephrine | 6.919 | 2899 | 0.140 | 12.180 | 13.4 |
| | Pseudoephedrin | 11.637 | 1560 | 0.244 | 21.166 | 12.3 |
| | Phenylpropanolamine | 13.776 | 1969 | 0.268 | 25.240 | 4.2 |
| **2.0** | **Acetaminophen** | **1.825** | **1769** | **0.079** | **2.443** | **-** |
| | **Guaifenisin** | **3.341** | **2687** | **0.071** | **5.303** | **10.1** |
| | **Phenylephrine** | **5.842** | **2847** | **0.109** | **10.022** | **13.9** |
| | **Pseudoephedrin** | **9.178** | **1541** | **0.174** | **16.328** | **4.1** |
| | **Phenylpropanolamine** | **10.505** | **1967** | **0.198** | **18.843** | **3.6** |
| 2.5 | Acetaminophen | 1.843 | 2031 | 0.072 | 2.477 | - |
| | Guaifenisin | 3.363 | 2683 | 0.071 | 5.345 | 10.6 |
| | Phenylephrine | 5.850 | 2761 | 0.116 | 10.082 | 13.3 |
| | Pseudoephedrin | 9.146 | 1533 | 0.184 | 16.527 | 11.0 |
| | Phenylpropanolamine | 10.398 | 1937 | 0.198 | 18.619 | 3.2 |
| 3.0 | Acetaminophen | 1.821 | 2005 | 0.062 | 2.436 | - |
| | Guaifenisin | 3.613 | 2687 | 0.093 | 5.817 | 11.6 |
| | Phenylephrine | 5.538 | 3003 | 0.109 | 9.449 | 9.5 |
| | Pseudoephedrin | 8.418 | 1668 | 0.172 | 14.883 | 10.2 |
| | Phenylpropanolamine | 9.446 | 2057 | 0.179 | 16.823 | 2.9 |
| 4.0 | Acetaminophen | 1.844 | 2430 | 0.051 | 2.479 | - |
| | Guaifenisin | 2.918 | 1932 | 0.075 | 4.506 | 8.5 |
| | Phenylephrine | 5.160 | 1157 | 0.175 | 8.736 | 8.9 |
| | Pseudoephedrin | 7.489 | 793 | 0.146 | 13.130 | 7.3 |
| | Phenylpropanolamine | 8.149 | 450 | 0.157 | 14.375 | 1.7 |

**Table 3.45** Effect of Flow rate

| Flow rate (ml min$^{-1}$) | Drugs | Chromatographic behaviors | | | | |
|---|---|---|---|---|---|---|
| | | $t_R$ (mins) | Area (mAU *s) | $W_{1/2}$ (min) | k′ | Rs |
| 0.8 | Acetaminophen | 2.390 | 2053 | 0.061 | 3.509 | - |
| | Guaifenisin | 4.316 | 2328 | 0.098 | 7.143 | 12.1 |
| | Phenylephrine | 7.601 | 2187 | 0.151 | 13.341 | 13.2 |
| | Pseudoephedrin | 11.786 | 2099 | 0.231 | 21.238 | 11.0 |
| | Phenylpropanolamine | 13.375 | 1134 | 0.240 | 24.236 | 3.4 |
| 0.9 | Acetaminophen | 2.124 | 2122 | 0.057 | 3.008 | - |
| | Guaifenisin | 3.833 | 2435 | 0.088 | 6.232 | 11.8 |
| | Phenylephrine | 6.757 | 2178 | 0.134 | 11.749 | 13.2 |
| | Pseudoephedrin | 10.479 | 2081 | 0.211 | 18.771 | 10.8 |
| | Phenylpropanolamine | 11.893 | 1172 | 0.222 | 21.440 | 3.3 |
| 1.0 | Acetaminophen | 1.908 | 2125 | 0.053 | 2.600 | - |
| | Guaifenisin | 3.442 | 2452 | 0.083 | 5.494 | 11.1 |
| | Phenylephrine | 6.072 | 2175 | 0.128 | 10.457 | 12.5 |
| | Pseudoephedrin | 9.420 | 2071 | 0.193 | 16.774 | 10.4 |
| | Phenylpropanolamine | 10.685 | 1165 | 0.204 | 19.160 | 3.2 |
| 1.1 | Acetaminophen | 1.734 | 2136 | 0.031 | 2.272 | - |
| | Guaifenisin | 3.124 | 2452 | 0.072 | 4.891 | 13.5 |
| | Phenylephrine | 5.513 | 2170 | 0.183 | 9.402 | 9.4 |
| | Pseudoephedrin | 8.821 | 1989 | 0.194 | 15.643 | 8.8 |
| | Phenylpropanolamine | 10.045 | 1078 | 0.211 | 17.953 | 3.0 |
| 1.2 | Acetaminophen | 1.605 | 2192 | 0.049 | 2.028 | - |
| | Guaifenisin | 2.978 | 2549 | 0.083 | 4.619 | 10.4 |
| | Phenylephrine | 5.254 | 2246 | 0.128 | 8.913 | 10.8 |
| | Pseudoephedrin | 8.356 | 1932 | 0.190 | 14.767 | 9.8 |
| | Phenylpropanolamine | 9.758 | 1073 | 0.212 | 17.396 | 3.0 |

**Table 3.45** Effect of flow rate (continued)

| Flow rate (ml min$^{-1}$) | Drugs | Chromatographic behaviors | | | | |
|---|---|---|---|---|---|---|
| | | $t_R$ (mins) | Area (mAU *s) | $W_{1/2}$ (min) | $k'$ | Rs |
| 1.3 | Acetaminophen | 1.497 | 2197 | 0.045 | 1.825 | - |
| | Guaifenisin | 2.861 | 2557 | 0.074 | 4.398 | 11.5 |
| | Phenylephrine | 5.055 | 2247 | 0.121 | 8.538 | 11.3 |
| | Pseudoephedrin | 8.180 | 1923 | 0.184 | 14.434 | 10.2 |
| | Phenylpropanolamine | 9.583 | 1068 | 0.201 | 17.081 | 3.6 |
| 1.4 | Acetaminophen | 1.394 | 2194 | 0.043 | 1.630 | - |
| | Guaifenisin | 2.657 | 2563 | 0.075 | 4.013 | 11.6 |
| | Phenylephrine | 4.693 | 2253 | 0.115 | 7.855 | 10.7 |
| | Pseudoephedrin | 7.593 | 1918 | 0.174 | 13.326 | 10.0 |
| | Phenylpropanolamine | 8.887 | 1066 | 0.189 | 15.768 | 3.6 |
| **1.5** | **Acetaminophen** | **1.296** | **2565** | **0.041** | **1.445** | **-** |
| | **Guaifenisin** | **2.471** | **2565** | **0.071** | **3.662** | **10.5** |
| | **Phenylephrine** | **4.370** | **2246** | **0.108** | **7.245** | **10.6** |
| | **Pseudoephedrin** | **7.081** | **1917** | **0.163** | **12.360** | **10.0** |
| | **Phenylpropanolami ne** | **8.280** | **1067** | **0.183** | **14.623** | **3.5** |
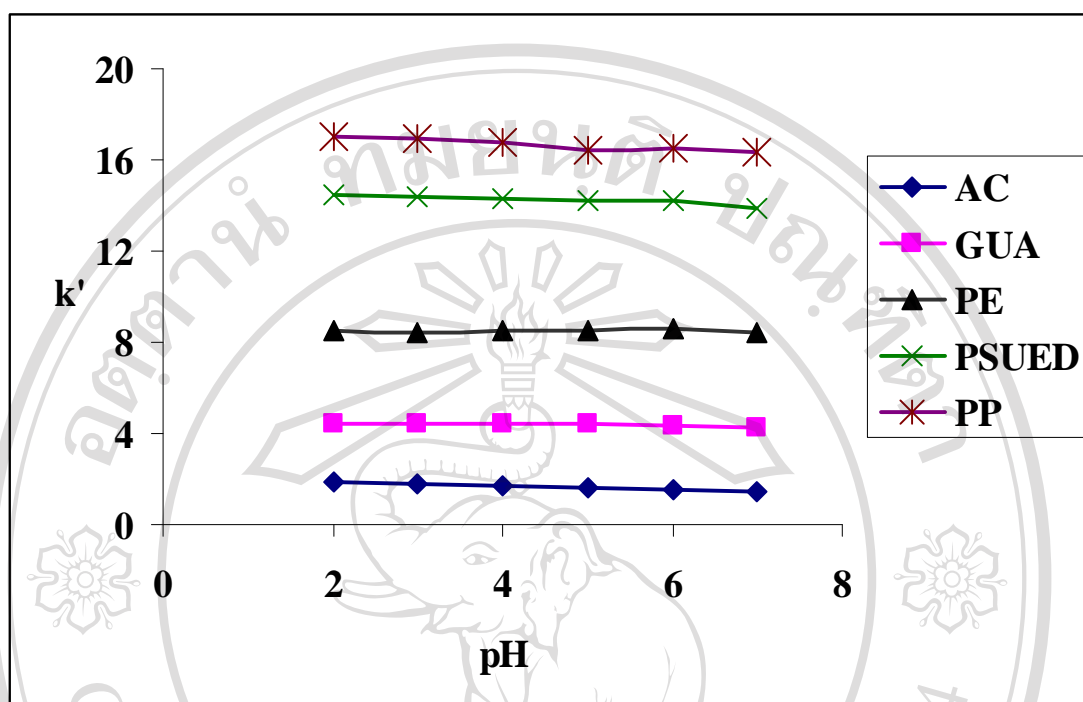
**Figure 3.31** Effect of pH on the retention acetaminophen (AC), guaifenesin(GUA), phenylephrine(PE), pseudoephedrine(PSUED) and phenylpropanolamine(PP). Micellar mobile phase: 0.150 mol l$^{-1}$ SDS, 2% v/v pentanol

### 3.3.2 Analytical Figures of Merit

#### 3.3.2.1 Linearity, Calibration Curve and Limit of Detection

Linearity is determined experimentally by analysis of a series of standards at five different concentrations that span at least 80–120% of the expected working range of the assay. Adamovich [258] recommended a range spanning 25–200% of the nominal range of analyte, using standards and spiked placebo samples. A linear regression equation obtained from the results should have an intercept not significantly different from zero; if it is, it should be demonstrated that this has no effect on the accuracy of

the method. In this investigation a linear plot was obtained from five different concentrations of working standard solutions using three replicate injections.

Calibration curves were constructed from triplicate injections of five solutions of each drug at increasing concentrations in the ranges 10–50 µg ml$^{-1}$ for phenylpropanolamine and pseudoephedrine (with a lower sensitivity) and 1–25 µg ml$^{-1}$ for the other drugs. The regression line was calculated as $Y = aX + c$ , where $X$ was the analyte concentration (µg ml$^{-1}$) and $Y$ was the response (peak area expressed as mAU * s). The linear regression coefficients ($R^2$) were always higher than 0.999. Table 3.46 lists the sensitivities (slopes of the calibration curves) and intercepts for 0.150 mol l$^{-1}$ SDS – 2.0 % pentanol with flow rate of 1.5 ml min$^{-1}$. The calibration curves of these drugs are shown in Figure 3.32- 3.36.

Limits of detection (LOD) and quantification (LOQ) were obtained for acetaminophen, guaifenesin, phenylephrine, pseudoephedrine and phenylpropanolamine according to the 3σ criterion and the 10σ criterion, respectively (Table 3.46). The results were based on the standard deviation of the response and the slope of a specific calibration curve containing the compound in a range of concentrations close to the LOQ. LOD and LOQ values are good enough to monitor the compounds under study in drug matrices.

**Table 3.46** Characteristic parameters of the calibration equations, LODs and LOQs

for the proposed method for simultaneous determination of five drugs

| Compounds | Conc. range ($\mu$g ml$^{-1}$) | slope | Intercept | $r^2$ | LOD ($\mu$g ml$^{-1}$) | LOQ ($\mu$g ml$^{-1}$) |
|---|---|---|---|---|---|---|
| Ace. | 1 – 25 | 64.62 ± 0.74 | 0.25 ± 1.32 | 0.9995 | 0.04 | 0.15 |
| Guai. | 1 – 25 | 70.36 ± 0.37 | 0.03 ± 3.03 | 0.9998 | 0.3 | 1.2 |
| Phen. | 1 – 25 | 49.79 ± 0.32 | 0.11 ± 2.57 | 0.9996 | 0.1 | 1.0 |
| Pseudo. | 1 – 50 | 22.19 ± 0.07 | 0.01 ± 2.33 | 0.9998 | 0.6 | 1.4 |
| PhenPro. | 1 - 50 | 49.79 ± 0.16 | 0.15 ± 0.52 | 0.9995 | 0.7 | 1.6 |

Ace. = Acetaminophen

Guai. = Guaifenesin

Phen. = Phenylephrine

Pseudo. = Pseudoephedrine

PhenPro. = phenylpropanolamine
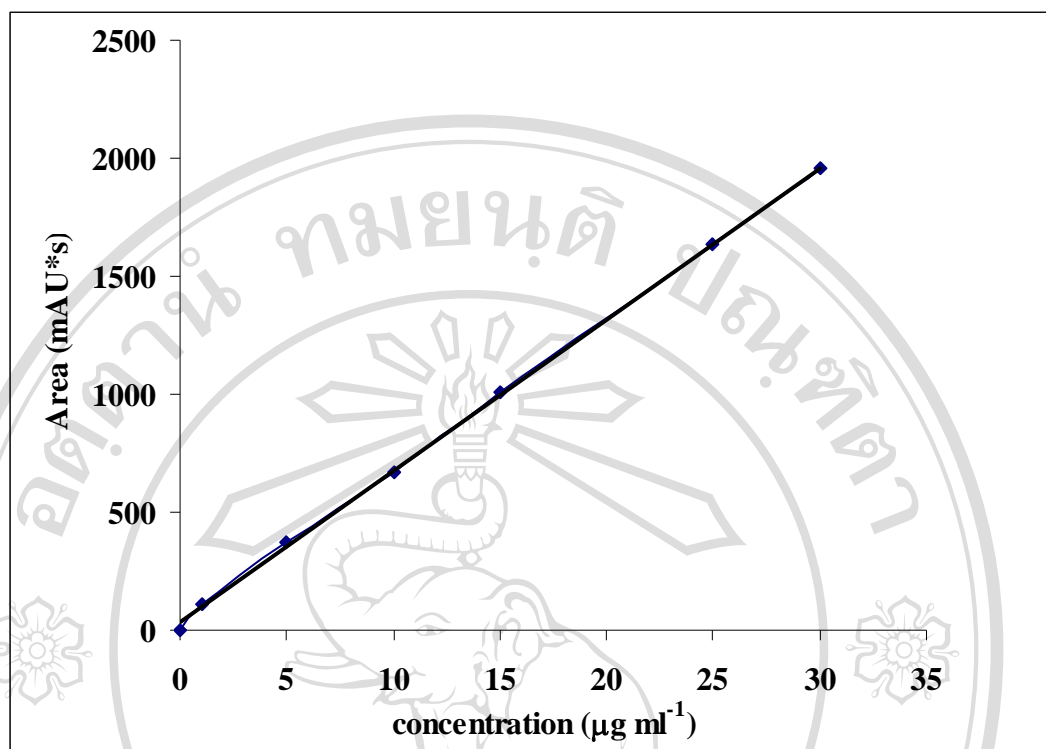
**Figure 3.32** Calibration curve for acetaminophen
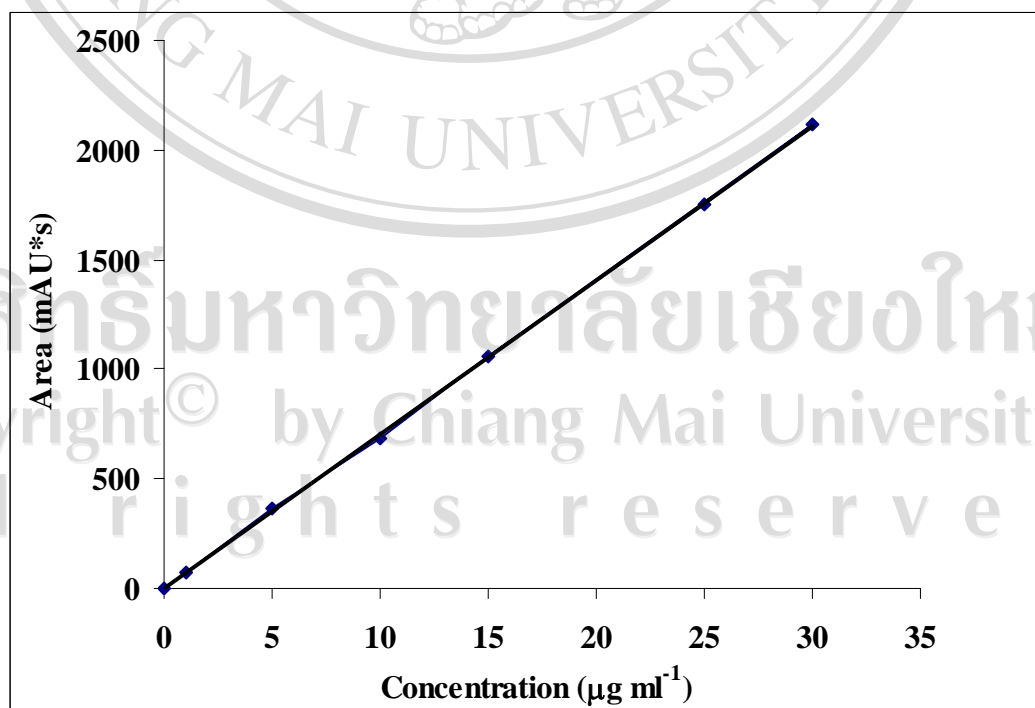


**Figure 3.33** Calibration curve for guaifenesin
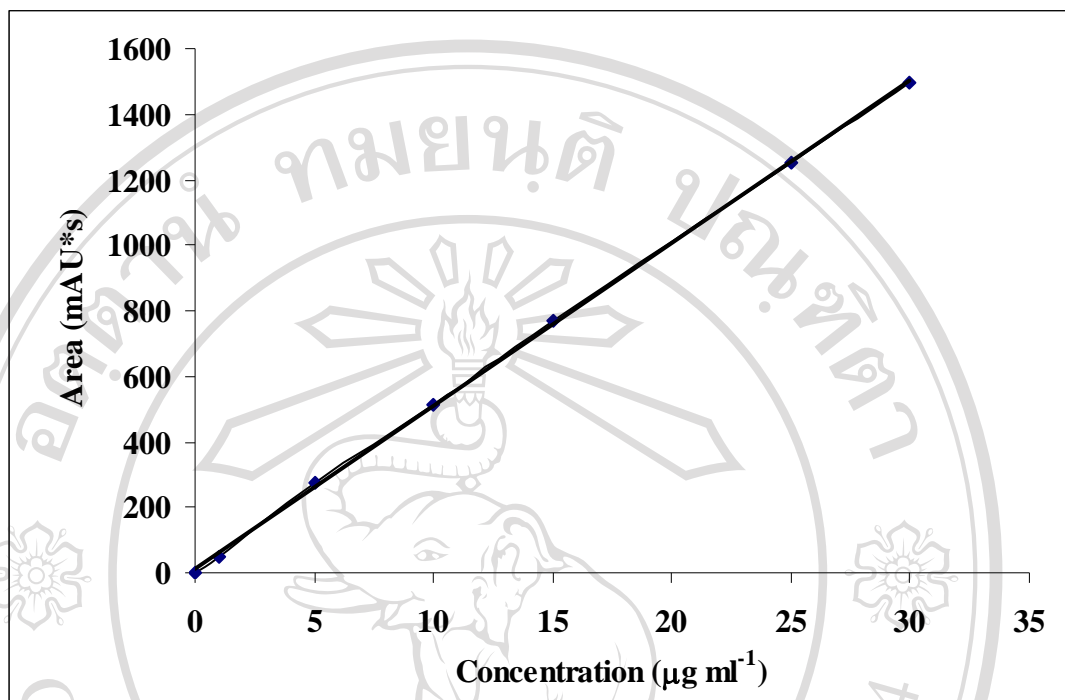
**Figure 3.34** Calibration curve for phenylephrine
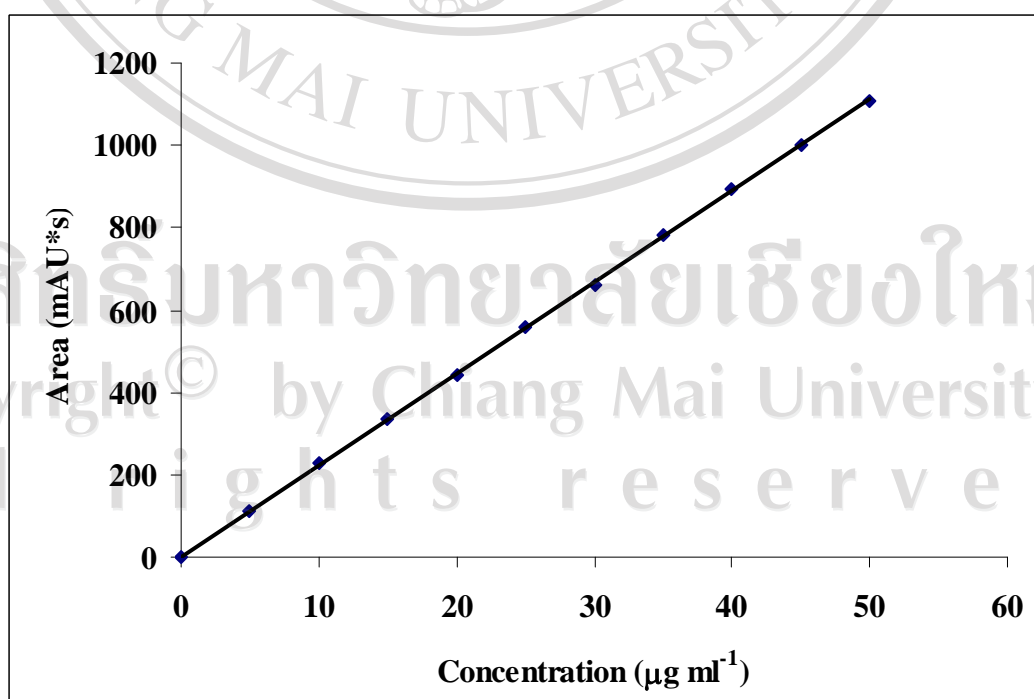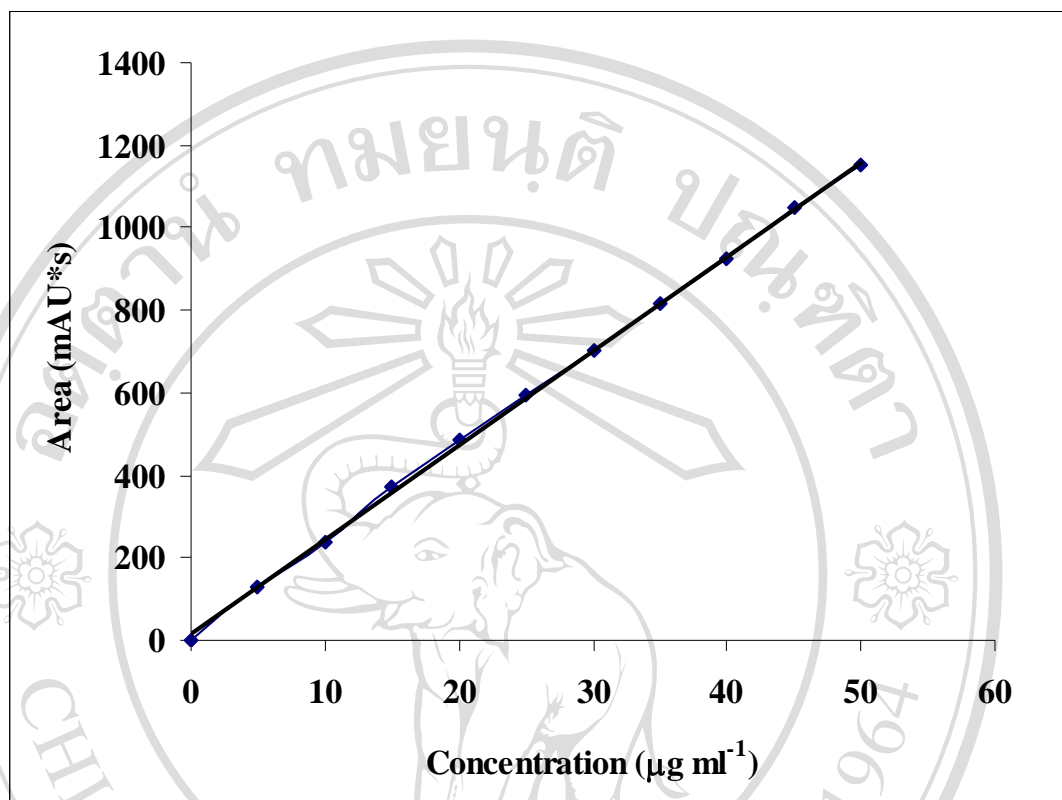
**Figure 3.35** Calibration curve for pseudoephedrine



**Figure 3.36** Calibration curve for phenylpropanolamine

### 3.3.2.2 Precision

The precision as intra-day and inter-day reproducibility, expressed as RSD %, was characterized by the spread of the data from replicate determinations. For the intra-day reproducibility, i.e. repeatability, ten determinations covering the specified range for the proposed methods on the same day were performed. Reference standard solutions were analyzed (triplicates each). Inter-day precision of the method was checked on ten consecutive days, by preparing and analyzing reference standard solutions under the same conditions. The results obtained from these analyses are listed in Table 3.47 as mean recovery. The Tables 3.47 – 3.48 show there were no

significant differences between assay results of either within-days or between days,

implying that the reproducibility of the MLC method was good.

**Table 3.47** Intra – day repeatability for the five drugs (% RSD, n = 10)

| Compounds | Intra – day repeatability | | |
|---|---|---|---|
| | 10 μg ml$^{-1}$ | 15 μg ml$^{-1}$ | 20 μg ml$^{-1}$ |
| Acetaminophen | 1.42 | 1.25 | 2.05 |
| Guaifenesin | 1.31 | 1.45 | 0.95 |
| Phenylephrine | 1.12 | 1.25 | 1.07 |
| Pseudoephedrine | 0.78 | 1.05 | 1.87 |
| phenylpropanolamine | 1.07 | 1.03 | 0.97 |

**Table 3.48** Inter – day repeatability for the five drugs (% RSD, n = 10)

| Compounds | Inter – day repeatability | | |
|---|---|---|---|
| | 10 μg ml$^{-1}$ | 15 μg ml$^{-1}$ | 20 μg ml$^{-1}$ |
| Acetaminophen | 1.45 | 1.37 | 1.12 |
| Guaifenesin | 1.17 | 1.06 | 0.97 |
| Phenylephrine | 1.05 | 1.78 | 1.95 |
| Pseudoephedrine | 1.07 | 1.15 | 1.11 |
| phenylpropanolamine | 1.94 | 1.17 | 2.09 |

### 3.3.2.3 Stability

The stability of stock standard of five drugs at 1000 μg ml$^{-1}$ was studied by storing at room temperature (25 -30 $^{o}$C) for seven days. Each standard solution was analyzed after dilution to 20 μg ml$^{-1}$ and the amount of each drug was calculated by comparing the peak area with that of the freshly prepared standard solution each day of assay at the same concentration and conditions. It was found that the solutions were stable over period of at least seven days at room temperature (Figure 3.37).
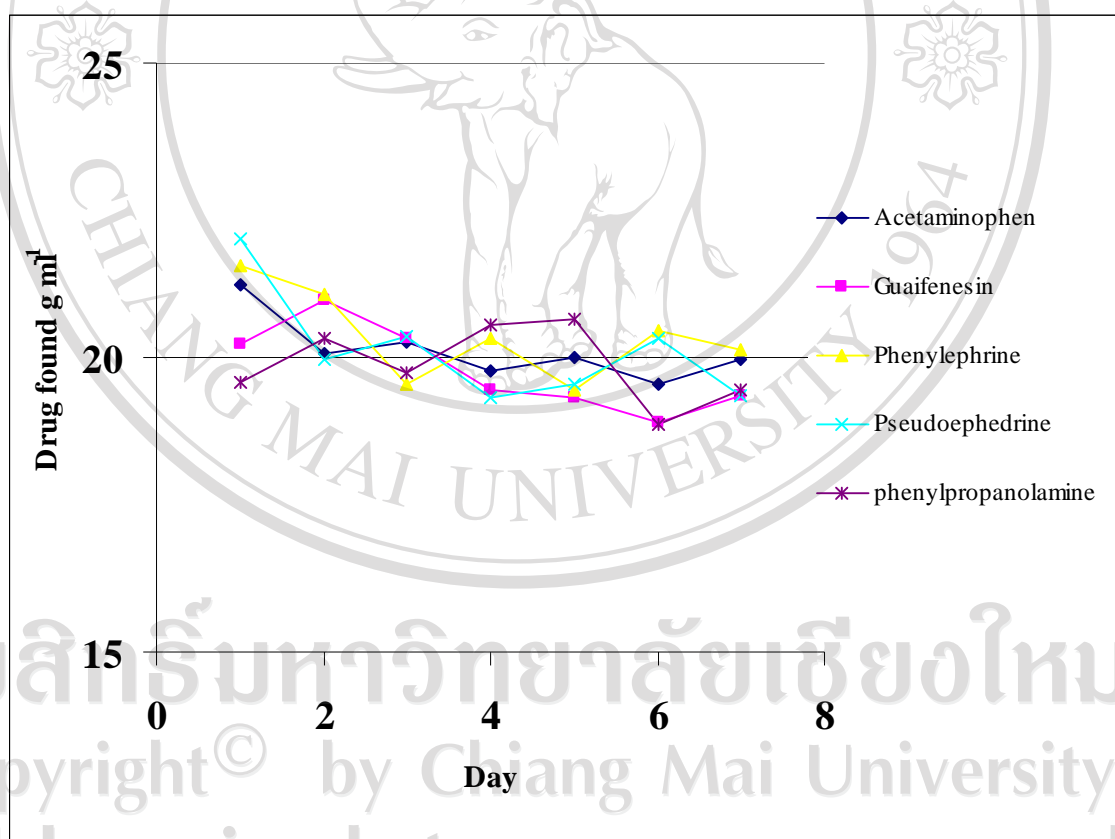


**Figure 3.37** Stability study at room temperature of 20 μg ml$^{-1}$ five drugs

### 3.3.2.4 Accuracy

The accuracy of the proposed method was determined from addition of known amounts of the studied compounds to a known concentration of the commercial pharmaceutical syrup (standard addition method). The resulting mixtures were analyzed by the proposed MLC method and the results obtained were compared with the expected results. The excellent recoveries of standard addition method suggested good accuracy of the proposed method (Table 3.49).

**Table 3.49** Accuracy results for five drugs analysis by MLC

| Sample | Acetaminophen | | | Sample | Guaifenesin | | |
|---|---|---|---|---|---|---|---|
| No. | Added µg ml^{-1} | Founded [a] µg ml^{-1} | % Recovery | No. | Added µg ml^{-1} | Founded [a] µg ml^{-1} | % Recovery |
| 1 | 15 | 14.86 | 99.07 | 1 | 15 | 15.27 | 101.80 |
| 2 | 20 | 20.13 | 100.65 | 2 | 20 | 20.11 | 100.55 |
| 3 | 25 | 24.89 | 99.56 | 3 | 25 | 25.19 | 100.76 |
| Sample | Phenylephrine | | | Sample | Pseudoephedrine | | |
| No. | Added µg ml^{-1} | Founded [a] µg ml^{-1} | % Recovery | No. | Added µg ml^{-1} | Founded [a] µg ml^{-1} | % Recovery |
| 1 | 15 | 15.13 | 100.87 | 1 | 15 | 14.77 | 98.47 |
| 2 | 20 | 20.21 | 101.05 | 2 | 20 | 20.14 | 100.70 |
| 3 | 25 | 24.93 | 99.72 | 3 | 25 | 24.89 | 99.56 |

### 3.3.3 Interference Study

Interferences were studied by injecting the solution of other drugs and other ingredients in formulation such as dextromethorphan. It was found that dextromethorphan presented the peak at retention time 3.886. Thus, it interfere phenylephrine peak ($t_r$ = 3.991), surprisingly, in any cold- cough drug containing phenylephrine, either dextromethorphan or phenylephrine was not found. Chlorpheniramine showed the peak at retention time more than 10 minutes so it did not interfere with the analyte peaks.
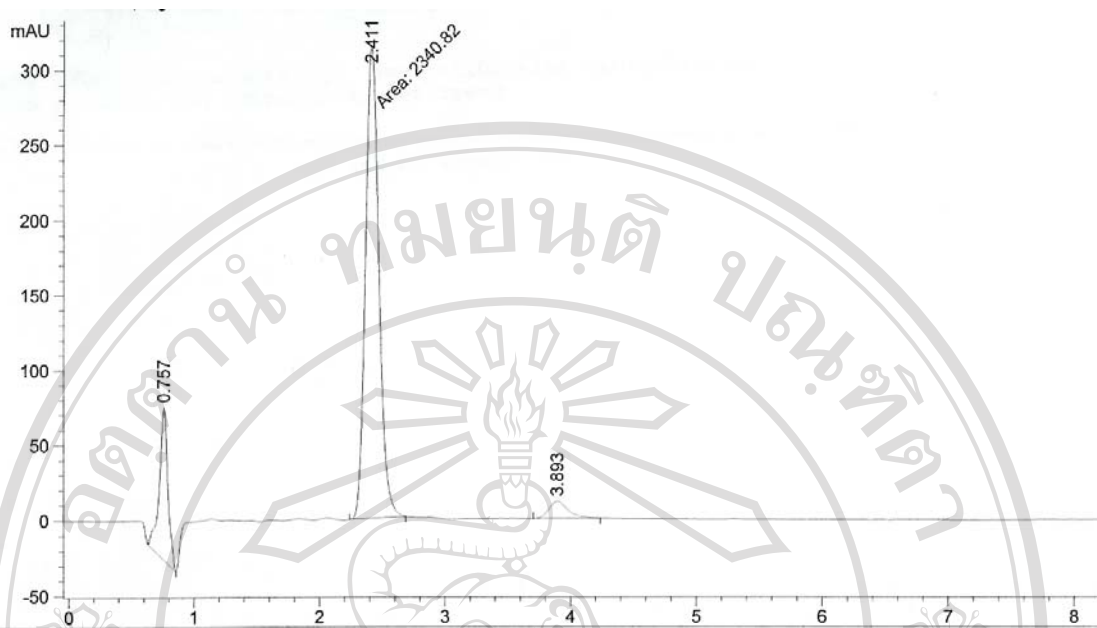
### 3.3.4 Analysis of Pharmaceutical Preparations

The optimized procedure was applied to the analysis of several combinations of the studied cough – cold drug in USA (acetaminophen, guaifenesin, phenylephrine, pseudoephedrine and phenylpropanolamine) (Table 3.50). These pharmaceuticals were analyzed using 0.150 mol $ml^{-1}$ SDS–2.0 % pentanol, with analysis times less than10 min. Each solution was analyzed by three independent determinations and each series were injected three times. The results were compared with those obtained with an RPLC procedure using 55% methanol at pH 7 at pH 210 nm. This mobile phase was optimized in this work for these separations. Chromatograms of some samples were shown in Figure 3.38 There was no significant difference by t-test between the mean values obtained from both methods at 95 % confidential limit.

**Table 3.50** Comparative analysis of pharmaceuticals with micellar and aqueous–organic reversed-phase liquid chromatography

| Pharmaceuticals | Compositions | micellar | | Aqueous - organic | | t-test |
|---|---|---|---|---|---|---|
| | | Found (mg) | RSD (%) | Found (mg) | RSD (%) | |
| Triaminic (syrup) | Each 5 ml contains: | | | | | |
| | acetaminophen (160 mg) | 160.36 | 0.72 | 159.85 | 0.65 | 0.24 |
| | dextromethorphan(7.5 mg) | | | | | |
| | pseudoephedrine (15 mg) | 15.22 | 2.52 | 15.01 | 2.60 | 0.20 |
| Robitussin® (syrup) | Each 5 ml contains: | | | | | |
| | dextromethorphan(10 mg) | | | | | |
| | guaifenesin (100 mg) | 100.45 | 1.18 | 99.96 | 1.36 | 0.28 |
| Daytime (Top CARE®) | Each 15 ml contains: | | | | | |
| | acetaminophen (325 mg) | 324.94 | 0.37 | 324.66 | 0.43 | 0.37 |
| | dextromethorphan (10 mg) | | | | | |
| | pseudoephedrine (30 mg) | 30.36 | 3.07 | 30.54 | 4.26 | 0.41 |
| Robitussin® (capsule) | Each capsule contains: | | | | | |
| | dextrominophan (10 mg) | | | | | |
| | guaifenesin (200 mg) | 200.71 | 0.79 | 201.18 | 0.75 | 0.32 |
| | pseudoephedrine(30 mg) | 29.92 | 3.31 | 31.21 | 2.67 | 0.03 |

**Table3.50** (continued)

| Pharmaceuticals | Compositions | micellar | | Aqueous - organic | | t-test |
|---|---|---|---|---|---|---|
| | | Found (mg) | RSD (%) | Found (mg) | RSD (%) | |
| Alka-Seltzer Plus® (tablets) | Each tablet contains: acetaminophen(250 mg) chlorpheniramine(2 mg) phenylephrine (5 mg) | 250.44 3.95 | 4.88 0.39 | 250.19 4.50 | 4.98 0.42 | 0.36 0.24 |
| Sudafed® (Capsule) | Each capsule contains: guaifenesin (200 mg), pseudoephedrine(30 mg) | 199.43 29.17 | 0.28 2.23 | 199.12 28.93 | 0.60 3.70 | 0.30 0.34 |

**(a)** Robitussin® (syrup)
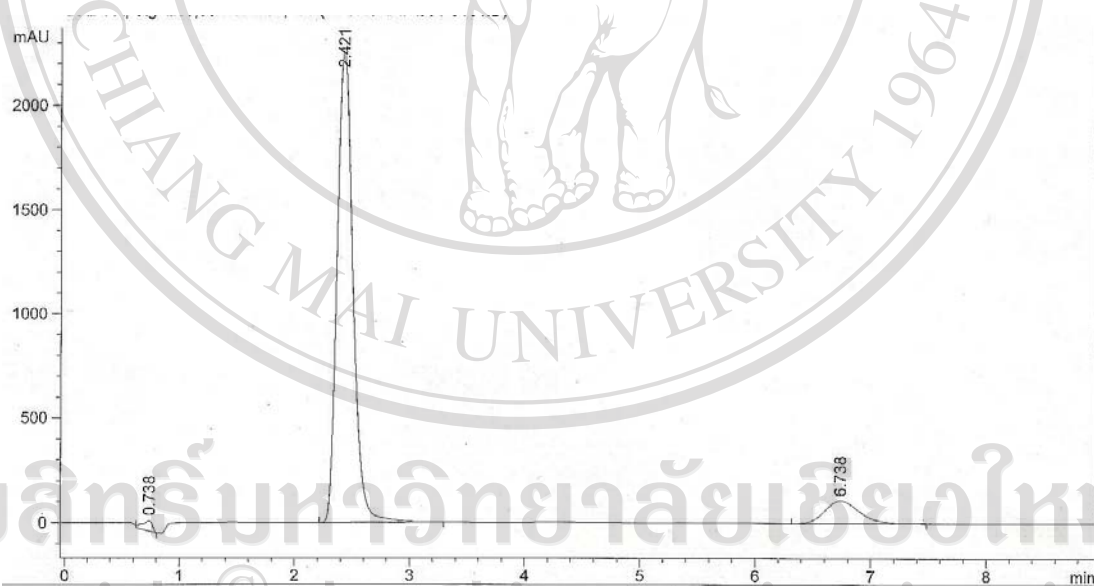


**(b)** Sudafed® (Capsule)
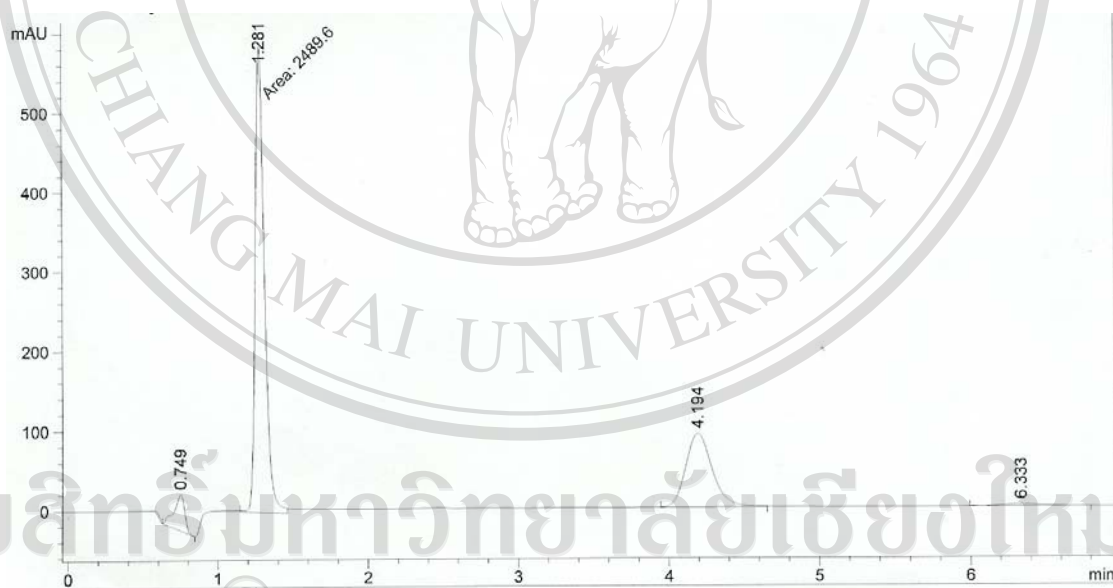
**(c)**Triaminic (syrup)



**(d)** Alka-Seltzer Plus® (tablets)

**Figure 3.38** Chromatograms of some pharmaceutical preparations (see Table 3.51).
**(a)** Robitussin® (syrup), **(b)** Sudafed® (Capsule), **(c)**Triaminic (syrup) and **(d)** Alka-

Seltzer Plus® (tablets)